DEVELOPMENT OF ELECTROSPUN SYNTHETIC BIOABSORBABLE FIBERS FOR A NOVEL BIONANOCOMPOSITE HERNIA REPAIR MATERIAL

A Thesis presented to

the Faculty of the Graduate School

at the University of Missouri

In Partial Fulfillment

of the Requirements for the Degree

Master of Science

---

by

J TODD VASSALLI

Dr. Sheila Grant, Thesis Supervisor

DECEMBER 2008

The undersigned, appointed by the dean of the Graduate School, have examined the thesis entitled

DEVELOPMENT OF ELECTROSPUN SYNTHETIC BIOABSORBABLE FIBERS FOR A NOVEL BIONANOCOMPOSITE HERNIA REPAIR MATERIAL

presented by J Todd Vassalli,

a candidate for the degree of Master of Science,

and hereby certify that, in their opinion, it is worthy of acceptance.

Dr. Sheila Grant, Biological Engineering Dept.

Dr. Fu-Hung Hsieh, Biological Engineering Dept.

Dr. Bruce Ramshaw, Dept. of Surgery

ACKNOWLEDGEMENTS

I would like to thank Dr. Sheila Grant for allowing me to be a member of her laboratory both as an undergraduate and graduate student. My experience in her lab has exposed me to a wide breadth of biomedical engineering research, which has been invaluable in my exploration of the field. Additionally, she has supported all of my academic endeavors, even the pursuit of a career in medicine, and I express sincere gratitude for her guidance and encouragement over the past few years.

I would also like to thank all of the graduate students in Dr Grant's lab. Their counseling has exponentially advanced my knowledge in biomedical engineering and has allowed me to be a productive member in the lab. I will, especially miss the daily conversations with my peers in room 147. The friendly atmosphere and frequent anecdotes have made my tenure as graduate student more memorable.

TABLE OF CONTENTS

LIST OF FIGURES

LIST OF TABLES

Table Page

DEVELOPMENT OF ELECTROSPUN SYNTHETIC BIOABSORBABLE FIBERS FOR A NOVEL BIONANOCOMPOSITE HERNIA REPAIR MATERIAL

J Todd Vassalli

Dr. Sheila, Thesis Supervisor

ABSTRACT

In order to create a more durable and biocompatible hernia repair mesh, a novel bionanocomposite material based on the crosslinking of bioabsorbable polymer fibers to decellularized porcine diaphragm tissue is proposed. The first step in creating this bionanocomposite material is to develop a method to produce and functionalize bioabsorbable polymer fibers. Electrospinning was chosen for its effectiveness and cost efficiency in producing polymer fibers in the sub-micron range. For this project, an electrospinning solution consisting of the degradable polymer polycaprolactone is treated with the aminolyzing agent ethylenediamine in order to add amine groups to the resulting electrospun fibers. Amine-group functionalization is measured using FT-IR scans of electrospun test samples. The degree of sample functionalization is measured as a numeric area of the respective amine peaks from the resulting FT-IR absorbance graphs. Current research findings indicate that it is possible to produce functionalized polycaprolactone fibers in the sub-micron range based on this experimental method.

CHAPTER 1

INTRODUCTION TO HERNIA REPAIR MATERIALS

1.1 Why Materials are used to Repair Hernias

An abdominal wall hernia is manifested by the loss of vital structural tissue resulting in the failure to contain viscera and support the torso.[1] Independent of the severity or location of a hernia, the root of its cause lies in the destruction of the molecular and cellular matrix.[1] There exist numerous debates concerning the factors, preventative or not, that dispose a person to a hernia injury. The focus of this investigation, however, is not to expand on these debates, but to discuss the currently available methods for treatment and the ongoing research to improve those methods. More concisely, the topics discussed here more often refer to the various commercially available hernia repair materials soliciting their benefits and drawbacks.

Put very simply, hernia repair materials are utilized in the surgical treatment of hernias in order to re-strengthen the area around the injury. This requires, in effect, simulating the injured or destroyed molecular and cellular matrixes that initially caused the hernia formation. The desired outcome of a hernia repair is restoring the fascial layer of the abdominal wall.[2] Depending on the case, a synthetic or a biological material is selected by the surgeons to be used in the hernia repair. The selection of a specific hernia repair material gives surgeons some needed flexibility in hernia treatment; however, there are always compromises. For instance, synthetic meshes, though providing the necessary mechanical support of the hernia repair site, are subject to chronic inflammatory response.[2] Likewise, while biological meshes allow for tissue remodeling and integration over time, they are also susceptible to weakening or biodegrading before

complete integration of native tissue.[2] In addition, the choice between a synthetic mesh and a biologic hernia repair mesh does not yet have a set of standard guidelines to follow. The selection of a particular mesh often times depends on surgeon preference, cost, patient, or material availability.

Below, a brief, guided discussion of current synthetic and biologic hernia repair meshes is put forth. Specific examples of both synthetic and biologic meshes are provided in order to give an overview of their effectiveness in treating hernia sites.

1.2 Current Materials: Synthetics vs. Biologics

1.2.1 Synthetics

The major benefit to using a hernia repair mesh is to decrease recurrence[3], thus reducing the risk of multiple surgeries and painful patient recoveries. It is well known that many synthetic polymer meshes have lower recurrence rates compared to suture repair.[4] Therefore, synthetic meshes thus far have been at the forefront of hernia repair since the inception of hernia repair materials in the 1950s.[3]

The one material that has been the standard for hernia repair material is Polypropylene.[3] Polypropylene, a nonabsorbable polymer, is noted for exceptional tensile strength comparable to that of steel[3], but the material is not without complications. The strength of polypropylene is far greater that what is required physiologically. Complications such as local wound infections, patient discomfort and restriction of the abdominal wall have occurred in patients with polypropylene hernia meshes.[4] Likewise, polypropylene meshes are well known for causing intestinal adhesions.[4] Another drawback is that polypropylene meshes oxidize and thus physical

and chemically degrade.[5] These meshes have been shown to shrink between 30-50%[3] after implantation, necessitating pre-placement calculations by the surgeons to achieve a correct fit. The overriding benefit of a polypropylene mesh, however, is that even with its propensity to incite infection, the infections themselves can often be treated without mesh removal.[3] Additionally, many of the risks associated with polypropylene can be modulated by adjusting mesh weight and porosity to promote more or less tissue in-growths. Though obviously not an inert material, polypropylene meshes are commonly employed by surgeons today.

Other non-absorbable polymers such as Polyester and Polytetrafluoroethylene (PTFE) are frequently used in synthetic hernia repair meshes. Polyester, a multifilament mesh composed of polyethylene terephalate, is chosen for hernia repair to improve conformability and tissue in-growth with the abdominal wall.[3] However, there are many problems associated with polyester meshes that currently limit there use in the United States. Frequently, Polyester meshes are subject to infection[6] and substantial loss of strength over time which can lead to and increased risk of hernia recurrence .[3] PTFE is a hernia repair mesh material that has smaller pores sizes compared to Polypropylene. While this property inhibits intestinal adhesion[7], it also does not facilitate tissue in-growth in the abdominal wall resulting eventually in encapsulation, thus a weaker hernia repair.[3] In addition, PTFE has been clinically shown to cause chronic infection which necessitates mesh removal.[8] The complications associated with both Polyester and PTFE meshes from the clinical uses have exposed a need for a better mesh material, such as a combination mesh material.

A combination mesh material combines the abdominal wall tissue in-growth property of Polyester meshes, while preventing the occurrence of intestinal adhesions associated with PTFE. Many manufactures have developed various combination mesh materials in attempt to provide surgeons with an improved synthetic mesh. Some manufactures have created hernia repair meshes that consist of both Polyester and PTFE for this very reason. A more recent movement in the design of combination synthetic meshes is to construct a mesh consisting of a Polypropylene or Polyester base coated with absorbable polymers. Clinical evidence show that bowel adhesion formation with hernia meshes usually occurs within a week of the initial surgery.[3] Thereafter, a layer of peritoneal cells coat the mesh and prevent the further risk of adhesion formation.[9] This finding suggests that synthetic meshes only need a temporary adhesion barrier, hence the use of absorbable polymer coatings. Conflicting results, however, do not provide enough corroborative data to currently determine which type of combination mesh performs the best in the clinical setting.

Yet another movement in the development of synthetic hernia repair meshes is to create materials consisting of 100% absorbable materials. Currently, there is not significant clinical data available to determine the viability of absorbable meshes. A possible benefit to using completely absorbable meshes is their use in contaminated fields, since they would not need to be removed and therefore could be placed in direct contact with the bowel.[3] Another potential benefit of absorbable meshes is the formation of a collagen layer upon healing. According to preliminary studies with the absorbable polymer polyglactin 910, however, the replacement collagen layer is not strong enough to prevent hernia recurrence and often results in catastrophic failure.[10]

Also, it is extremely important to achieve polymer degradation rates that are in sync with tissue in-growth. Although not particularly promising as a stand-alone material, absorbable synthetic polymers with the ability to remodel tissue may lead into a novel direction for hernia repair materials.

1.2.2 Biologics

As mentioned before, the ultimate goal of hernia repair is to completely restore the fascial layer of the abdominal wall. Currently available synthetic mesh materials do not achieve this. Permanent non-degradable synthetic meshes commonly cause chronic inflammation, scar formation, loss of compliance, and chronic pain.[2] Likewise, chronic infection frequently plagues many synthetic mesh materials once implanted at the hernia site. Clinical explants of synthetic hernia meshes do not show vascular in-growth, which would normally work to clear infection.[2] To address the problems associated with synthetic mesh designs, there has been a shift into exploring biologics as a better alternative. Ideally a biological mesh is engineered first to provide the necessary mechanical support at the hernia repair site.[2] This then allows time for new tissue to gradually remodel along the mesh scaffold in order to create a network of organized collagen and establish new vascular access to the site.[2] Current biological mesh materials are derived from a number of different sources, but there exits a common theme among these different products. Base materials for biologic meshes are chosen from collagen rich tissues and then are stripped of all cellular contents, leaving behind the collagen scaffold along with extracellular ground matrix structures.[2] The resulting

material may or may not undergo further modification before being used as a hernia repair mesh.

The use of xenogeneic extracellular matrix (ECM) materials as tissue engineering scaffolds is not a novel concept. Tissue scaffolds have been employed in the repair and reconstruction of many different body tissues including musculoskeletal, cardiovascular, urogenital and itegumentary structures.[11] Decellularization of both xenogeneic and allogeneic tissues is a necessary first step in producing a viable biologic hernia repair matrix. The reason for this being that the cellular antigens from the original tissue are recognized as foreign by the host and facilitate both an inflammatory response and immune-medicated rejection of the implanted material.[12] After decellularization of the original tissue, there are a number of very useful components left behind in the extracellular matrix (ECM) that are well tolerated even by xenogeneic recipients.[13, 14] The beneficial components remaining in the decellularized ECM include a complex agglomeration of structural and functional proteins, glycosaminoglycans, glycoproteins, and numerous other small molecules and growth factors.[15, 16] These residual components give the decellularized ECM the unique property of modulating a wound healing response instead of facilitating scar tissue formation.[11]

The collagen biopolymers currently marketed and used as hernia repair products include skin, fascial structures, and the intestinal submucosa layer.[2] Several products have been developed and a few are briefly discussed here. Surgisis Gold, first developed at Purdue University in 1987, is an ECM mesh obtained from the submucosa layer of porcine jejunum.[2] Surgisis Gold is produced by layering together 4-8 sheets of porcine small intestinal submucosa to provide a thicker lamination for increased strength.[2]

According to clinical studies, Surgisis promotes rapid cellular in-growth and cell differentiation which results in the healed tissue closely resembling the host tissue.[17] A drawback to Surgisis is its tendency to delaminate if not kept moist.[17] Delamination carries the implication of reduced strength at the implant site, which if not completely healed could cause failure.

Permacol engineered by Tissue Science Laboratories, Inc. (TSL) is another product that is utilized as a biologic hernia mesh material. Permacol is a porcine acellular full thickness dermis tissue that is crosslinked with hexamethylene diisocyanate. Although dermal tissue is more frequently associated with skin grafts, favorable reports of reduced scarring, graft incorporation, and angiogenesis have prompted acellular dermis use in hernia meshes as well. The chemical crosslinker in Permacol inhibits the ability of collagenase from binding to its site specific area on the collagen molecule and thus delays or prevents mesh digestion.[2] The crosslinker provides protection against premature mesh degradation thus ensuring that the product has the necessary mechanical strength during the wound healing process. The problem with crosslinking a biologic in certain situations is the possibility of inciting foreign body reaction which would cause encapsulation instead of tissue integration.[2]

One example of fascial structures being used as hernia repair meshes is a product called Veritas developed by Synovis Surgical. Veritas is produced from an acellular bovine pericardium. Preliminary data show that the mesh resists adhesion formation and within one month of mesh implantation there is significant host tissue remodeling of the scaffold.

Although biologic meshes show great promise a hernia repair meshes, currently surgeons are hesitant to select them over synthetic hernia mesh materials. The primary reason that biologics have not yet gained wide acceptance is their rookie status as hernia meshes. Many surgeons are more comfortable working with synthetic meshes due to their familiarity within the field and ample clinical research data that permits a scientific predictability in performance. Additionally, some surgeons remain skeptical of biologic meshes due to reports of higher mechanical failure compared with synthetic meshes. Also, there looms the possibility of disease transmission with biologics meshes, however, no reports on disease transmission are currently published.[2] Many of these worries with biologics should eventually be quelled with more advanced research and clinical trials.

1.3 Current Research: Bionanocomposites

With all of the problems associated with current hernia mesh designs, researchers and clinicians have put together a list of properties that an ideal mesh should possess. These properties include long-term resistance to physiological stresses, pliability with the abdominal wall, facilitation of tissue in-growth, resistance to bowel adhesions, inhibition of foreign body reactions, resistance to infection, and possession of non-carcinogenic properties.[7]' [18] Neither synthetics nor biologics possess all of these properties. The hope is to advance the viability of biologic hernia meshes at the implant site. Some biologic hernia meshes possess all of the properties of the ideal mesh described above with the exception of the ability to withstand long term physiological stresses. We have

proposed new research with the aim to create material that remedies the deficiencies of biologic meshes. Our solution is in the form of bionanocomposite materials.

The infusion of synthetic nanomaterials such as polymer nanofibers and nanotubes into decellularized ECM tissue scaffolds constitutes the making of a bionanocomposite material. Polymer nanofiber and nanotube systems can be chosen so that favorable interactions can occur between the biological and synthetic constituents.[19] The introduction of synthetic nanomaterials allows a bionanocomposite material to be tightly controlled by the nature of the polymer and its internal physical morphology.[19] The implications of material with such properties are promising. In the case of hernia mesh repair materials, it may be possible to create bionanocomposite that modulates normal tissue healing, while providing the necessary mechanical strength to carry wound healing to completion.

CHAPTER 2

LITERATURE REVIEW

2.1 Introduction to Electrospinning

2.1.1 Electrospinning Overview

Electrospinning is a process developed by A. Formhals in 1934 to create polymer fibers via the electrostatic force.[20] Essentially, nanofibers (fibers smaller than the 500 nm) can be produced from either a polymer solution or melt utilizing a high voltage power supply, a metallic dispensing needle, and a grounded conductor for fiber collection.[21] Although the process of electrospinning was pioneered over seventy years ago, it did not gain much attention by the scientific community until the 1990s when its applications became readily apparent. Electrospinning has since found its niche in the field of tissue engineering. Since the mid nineties, hundreds of research papers have been published detailing the process of electrospinning and its potential applications in tissue engineering.

Tissue engineering by definition is a field that seeks to create or repair damaged tissues and organs by fabricating materials consisting of a mixture of cells, biomaterials, and biologically active molecules.[22] Polymer nanofibers produced from electrospinning have been found to improve the process of tissue regeneration in tissues such as bone, cartilage, cardiovascular tissue, and nerves.[23] Human cells proliferate around polymer nanofibers since the fibers have diameters that are smaller than the cells that they anchor.[23] Specifically, electrospun polymer nanofibers can provide the necessary mechanical strength for host-appropriate cells populate the scaffold and deposit ECM components exclusive to the organ that is targeted for repair.[22] An ideal scaffold

for tissue for tissue engineering approximates the structural morphology of a tissue's natural collagen network.[22] Essentially, the ideal tissue scaffold has sufficient porosity, surface area, and surface chemistry to permit cell adhesion, growth, migration, and differentiation as well as an appropriate degradation rate to match the rate of regeneration of the natural tissue.[22] Current research with electrospun fibers focuses on achieving this goal. With that said, there are numerous parameters that dictate the morphology of electrospun nanofibers that need to be addressed in order to grasp the complexity of the seemingly simple process of electrospinning.

2.1.2 Parameters Controlling Fiber Morphology

As briefly mentioned in the previous subsection, electrospinning is a process that results in the production of polymer nanofibers. This process is achieved by applying a high voltage source to a polymer solution causing charges to build up in a droplet of solution to form a conical deformation known as a Taylor cone. At a certain threshold, a polymer jet is ejected from the cone deformation and travels to a region of reduced electrical potential, such as a grounded plate .[24] There are several parameters in the electrospinning process that influence resulting fiber morphology. Broadly defined parameters such as polymer solution, processing conditions, and the ambient environment will be discussed in expanded detail in order to become familiar with the complexity of electrospinning. When reviewing these parameters it is imperative to remember that numerous studies have be published detailing the effects of individual variables in electrospinning; however, there are no strong scientific principles that dictate the

electrospinning process on the whole. Most researchers readily admit that achieving specific electrospinning fiber morphology requires trail and error.[24]

Polymer solution parameters are the most influential in determining electrospun nanofiber morphology. Specifically, solution viscosity and surface tension are frequently referenced when discussing polymer solution parameters. Below, a brief discussion of viscosity and surface tension explains how both affect solution parameters and the resulting implications.

Solution viscosity is used both qualitatively and quantitatively in reference to the resistance of fluid deformation. It is generally understood that polymer molecular weight is correlated with polymer solution viscosity. As the molecular weight of a given polymer increases so does solution viscosity. The solution viscosity's dependence on molecular weight can be extrapolated to describe the degree of polymer entanglement during electrospinning.[24] Therefore, a higher solution viscosity results in more polymer entanglement, which serves to maintain a continuous jet during electrospinning.[24] Polymer solution concentration is also a determinant of solution viscosity, thus polymer entanglement during electrospinning.[24] Depending on its viscosity, a given polymer solution (polymer and solvents), can produce various fiber morphologies, while keeping all other parameters constant during electrospinning. For instance, results detailing an electrospinning experiment with polystyrene (m.w. 190,000 g/mol) dissolved in tetrahydrofuran showed that the transition between the bead-dominant fibers and bead- free fibers fell in the 18-35 wt% range for the polymer solution.[25] Qualitatively, these results are caused by the reduction in ejected polymer jet bending instability which results in a shorter jet path and less fiber stretching, hence

more uniform and larger diameter fibers.[26] Other studies show that there is a definite range of viscosities appropriate for electrospinning. If a solution viscosity is too high, then the electrospinning process may not occur at all; whereas a solution viscosity that is extremely low produces discontinuous polymer deposition instead of fibers.[27],[28]

Surface tension is another important solution parameter that determines the resulting electrospun fiber morphology. Surface tension is the intermolecular attraction of solution molecules that causes the surface solution to behave as an elastic sheet. In order to initiate electrospinning, the force of the surface tension must be overcome to form the polymer jet.[24] Likewise, solution viscosity plays an important role in determining the effects of surface tension. If a particular solution has a high viscosity, then solvent molecules spread more evenly over the entangled polymer. This in turn reduces the probability of solvent molecules to merge together, thus reducing surface tension.[24] Therefore, a reduction in surface tension reduces the beading of an electrospun fiber.[5, 24]

Electrospun polymer nanofiber morphology is also heavily dependent on processing conditions. These parameters encompass the controllable parameters of the electrospinning process outside the solution composition. Specifically, external factors such as voltage, electrode separation distance, type of collector, solution flow rate, temperature, and needle diameter all contribute to the overall outcome of electrospun fiber morphology.

Voltage in the electrospinning process can be compared to the effect that gravity has on a waterfall. High voltage contributes to the electrospinning process by creating the necessary electrostatic force in conjunction with the electric field to overcome

solution surface tension.[24] The higher the applied voltage, the more the columbic repulsive force will be present within the polymer jet causing greater stretching and a reduction of fiber diameter.[29] Correspondingly, it is not surprising that increases in voltage also increase the beading effect in the resulting fibers due to a more pronounced whip-like motion of the ejected fiber caused by the bending instability.[30] In addition, higher applied voltage increases the rate of solvent evaporation producing drier and more a distinguishable fibrous deposition as opposed to an interconnected mesh.[31] As with other electrospinning parameters, the voltage effects on fiber morphology are not standardized. The constant struggle to maintain the Taylor cone requires frequent adjustments to the voltages strength in conjunction to monitoring other electrospinning parameters. Therefore, there is always a careful balancing act on the part of the experimenter to obtain the desired fiber morphology.

Another important external factor leading affecting electrospun polymer fiber morphology in is electrode separation distance. The electrode separation distance refers to measured distance between the high potential voltage potential of the dispensing needle and the grounded collecting plate. The electrode separation distance contributes to the polymer fiber morphology by affecting flight time and electric field strength.[24] As electrode separation distance increases and electric field strength decreases, the flight time of the ejected polymer jet increases which gives more time for solvent evaporation and the formation of independent fibers.[24] Conversely, as electrode separation decreases, flight time shortens and the electric field strengthens allowing less time for solvents to evaporate. The resulting mat then resembles a conglomeration of fibrous junctions instead of individual fibers.[32]

Not often addressed when discussing electrospinning is the effects of the grounded collecting plate. The type of material chosen for the grounded collector determines the degree of surface charge build up during the electrospinning process. It has been demonstrated that polymer fiber deposition during electrospinning is inversely proportional to surface charge accumulation on the collector.[33] Therefore, a more highly conducting collecting plate is chosen to increase the density of the deposited electrospun nanofibers.

Solution flow rate must also be accounted for in the characterization of electrospun fiber morphology. Essentially, solution flow rate adjustments are made in order to maintain a stabilized Taylor cone during electrospinning.[24] To a certain extent, increasing the flow rate while maintaining the Taylor cone produces larger fiber diameters.[34] Increasing the flow rate too much causes fibers to be collected without sufficient solvent evaporation leading to flattened web-like appearance.[24] Optimally, a lower solution flow rate, while maintaining the Taylor cone is more ideal since it permits time for solvent evaporation and produces better fibers.[35] However, a solution flow rate below the threshold for a given voltage causes evaporation at the needle tip, thus preventing electrospinning.

Temperature effects on the electrospinning process are most influential on the properties of the polymer solution. Raising the temperature often results in both an increase in the evaporation rate of the solvent and a reduction in the polymer solution viscosity.[24] Similarly, raising the temperature, as in the case of polyethylene, permits more polymer solubility and more uniformity in the electrospinning process.[36] However, raising the temperature of natural protein biopolymers such as collagen can

cause denaturization, therefore room temperature conditions are better.[37] Selecting the correct temperature depends on the polymer and the solvent, and usually requires numerous trials to determine the optimal temperature to produce specific fiber morphologies.

The effect of needle diameter is another parameter in electrospinning that sometimes is overlooked. The needle diameter has great influence on the size and shape of the solution droplet. For instance, a smaller dispensing needle diameter produces a smaller, more compact droplet of solution, which subsequently increases surface tension.[24] The result of this effect is that a higher columbic force is needed for the same applied voltage, so when a polymer jet forms, the polymer undergoes a greater degree of stretching and elongation.[24] There is some compromise when choosing electrospinning needle diameters. While smaller diameters have shown to reduces needle clogging (due to solution exposure to the air)[38], diameters too small prevent more viscous solutions from being drawn out.

Surprisingly enough, when attempting to create electrospun polymer fibers with specific morphologies, the ambient environment plays a crucial role. Although the effect of the ambient environment on electrospun fiber morphology has not been explored in much detail, there are a few investigations concerning the effects of humidity and atmospheric draft that need to be discussed.

The effect of humidity on electrospun fiber morphology, though not the focus of many studies, is important enough to implement measures to monitor its level.[39] A few researchers have suggested that increased levels of humidity cause fluid condensation on the surface of electrospun fibers which works to form pores.[24] Likewise, obvious

effects of humidity include the rate of solvent evaporation. Lower ambient humidity causes a greater solvent evaporation rate compared to higher ambient humidity.[24] Humidity may also play a role in the amount of electrostatic charge the emerging polymer, effectively reducing charge accumulation at higher humidity levels.[24] Humidity can therefore affect not only fiber morphology, but also the deposition orientation.

Atmospheric draft is another ambient parameter that rarely is discussed with the electrospinning process. Slight changes in wind speed and direction, while electrospinning, affects the electrospinning process. For instance, change in wind speed causes a slight pressure gradient which can affect the stability of the electrospinning jet.[24] Altering the jet flow or position shapes both jet charging and electric field dynamics. Inconsistency in the charging and the resulting current within the jet strongly dictates resulting fiber diameter.[40] Therefore, unmonitored atmospheric draft lends itself to unpredictable fiber morphologies. One way to combat unstable atmospheric draft is to enclose the electrospinning apparatus, thus preventing unwanted wind currents from the ambient air.

2.2 Synthetic Degradable Polymers

The bioengineering field has placed much emphasis on the development of absorbable polymer scaffolds that can be used in tissue engineering.[41] These scaffolds should mimic the matrix profile of the surrounding tissue and promote a natural state of differentiation of the cellular components.[41] Electrospinning provides a means to construct nanoscale polymer fibers that resemble the extracellular matrix, but the

selection of polymer materials is just as vital in creating a bio-scaffold. Studies with synthetic absorbable polymers such as polylactic acid, polyglycolic acid, and polycaprolactone and their various co-polymers have demonstrated encouraging results in regard to tissue engineering.[41] This section details a few of these absorbable synthetic polymers by outlining their favorable properties to electrospinning and tissue engineering.

Polycaprolactone (PCL) has been a target polymer for electrospinning and tissue engineering over the past decade. PCL is attractive for is flexibility, biodegradability, and relatively hydrophobic nature.[42] In addition, as a synthetic polymer, PCL is ideal for electrospinning since it has a favorable glass transition temperature and melting point (Tg= -60 C; Tm= 60 C).[43] Electrospun PCL fibers are biocompatible and can be used in wide range of soft and hard tissue biomedical applications.[43] Likewise, since it has a relatively low rate of hydrolytic degradation, PCL is appropriate as a long term implantable material.[43] PCL is frequently employed as a constituent fiber material in tissue matrixes as it has been shown to support cell attachment and proliferation.[43] PCL's flexible nature also makes it an ideal polymer for integrated polymer tissues matrixes to increase mechanical durability. Tensile tests show that electrospun PCL fiber scaffolds absorb repetitive functional stress, which reduces the possibility of tissue failure due to fatigue or high stresses.[24] As with other absorbable synthetic polymers, the drawback to using PCL is the lack of control of degradation rate in the body. In order to be optimally effective in a bio-scaffold, PCL needs to promote cellular attachment and growth allowing normal healthy tissue to form while simultaneously degrading.[44] So the trick is to provide the necessary mechanical support to the bio-scaffold, and then

disappear to avoid interference with the newly formed tissue. Researchers readily admit that the science of biodegradation rates is far from perfect. Promising studies show that steps like producing varying forms of PCL co-polymers with other synthetic absorbable polymers such as polylactic acid allow for greater control of degradation rates.[45]

Polylactic acid (PLA) and polyglycolic acid (PGA) and respective co-polymer derivatives are used in addition to PCL to achieve specific electrospun fiber morphologies with predictable mechanical strength and degradation rates.[46] One of the most popular co-polymers produced from PLA and PGA is poly(lactide-co-glycolide) (PLGA). For instance, PLGA is approved by the Food and Drug Administration for use as a drug delivery polymer for antibiotics such as cefazolin for various tissue engineering applications[47]. The idea is that antibiotics embedded in PLGA can undergo a timely release during PLGA degradation to minimize infection at the site of an implant.[47] PLGA has also been coupled with the drug paclitaxel in studies that aim to treat cancerous brain tumors.[48] PLGA is a particularly good choice since its degradation products (PLA and PGA) undergo further enzymatic degradation and are metabolized by the citric acid cycle.[47]

Absorbable synthetic polymers are also frequently blended with naturally occurring polymers for forming electrospun bio-scaffolds. For example, PGA has been combined with collagen and glycosaminoglycans (GAGs) to construct bio-scaffolds that speed up tissue regeneration while providing superior mechanical strength.[49] Likewise, a study with a hybrid bio-scaffold using urinary bladder ECM and biodegradable polyurethane showed improved mechanic robustness and flexibility from the synthetic polymer and increased cell adhesion and proliferation from the natural

components.[50] Studies show that natural polymers, while they are the best at stimulating tissue regeneration, have poor *in vivo* mechanical strength.[49] The prohibitive costs of natural polymers coupled with their inferior mechanical strength necessitate the use of synthetic absorbable polymers to increase viability of electrospun bio-scaffolds.[49]

2.3 Polymer Functionalization

There are many potential applications for electrospun polymer nanofibers, especially in the field of tissue engineering. Unfortunately, degradable synthetic polymer fibers are chemically inert and require various forms of functionalization to improve biological viability.[24] For instance, polymer functionalizations help a polymer to attain more conducive surface properties such as a specific chemical composition, hydrophilicity, roughness, crystallinity, conductivity, lubricity, and crosslinking density.[24] Each type of polymer functionalization has its own unique purpose in creating specific tissue engineered products. Below, a few of these functionalization methods are discussed to provide an overview on their various processing methods. Keep in mind that the information provided is just a survey, and is not intended to be used as protocol.

One method used for degradable synthetic polymer functionalization is graft copolymerization due to its ability to create distinctive surface chemistries through the use of various monomers.[24] Essentially, this process involves forming radicals on the polymer surface, exposing the radicals to oxygen, then reacting with different monomers to obtain the desired result.[24] An example developed by one research group includes

the functionalization of poly-ε-caprolactone (PCL) with hydroxyl, carboxylic acid, or epoxy groups.[51] Essentially, α-chloro-caprolactone prepared by a Baeyer-Villiger oxidation was copolymerized with PCL followed by an atom transfer radical addition (ATRA) reaction using but-3-en-1-ol, vinylacetic acid, and 1,2-epoxyhex-5-ene.[51] The procedure resulted in various degrees of functionalization along the PCL polymer chains.[51] Another research group performed the direct grafting of PCL with maleic anhydride (MA) producing randomly crosslinked chains.[52] In this case, functionalization was performed by first adding PCL, peroxide, and MA to a melt reaction chamber, then adding glycidyl methacrylate to complete the graft.[52] Overall grafting methods are especially useful for synthetic degradable polymers since they are less susceptible to the effects of polymer degradation.[53]

Surface modification of degradable synthetic fibers also includes functionalization with naturally derived molecules like the peptide sequence arginine-glycine-aspartic acid (RGD).[54, 55] RGD sequences are often investigated since they trigger cell adhesion and permit cell line selectivity to promote specific cell responses.[54] A variety of different methods have been employed to attach RGD peptide sequences to degradable polymers. For example, one study used carbodiamide chemistry to create an aminated PCL surface in order to covalently attach the RGD sequence.[55] Another study involved the chemical immobilization of PCL with the RGD sequence by 4 stage reaction.[56] Initially, the PCL underwent isocyanation by hexamethylene diisocyanate. Subsequently, a hydrolysis reaction to obtain amino groups was performed by NaOH. Then the reacted polymer underwent activation by disuccinimidyl suberate, and finally RGD immobilization.[56] RGD sequences have also been used to covalently modify

blended degradable polymers.[57] A blend of PLGA and a PLGA-b-PEG-NH_2 diblock copolymer was first electrospun, then the free primary amine groups on the surface of the fiber were covalently linked after a reaction with the RGD sequence. While not listed here, RGD immobilization can be induced by countless other crosslinking protocols, and the RGD peptide sequence is just one of many peptide sequences used to promote cellular growth in tissue scaffolds.

Aminolysis was briefly referenced during the discussion of RGD immobilization, but it deserves a bit more attention due to its importance in degradable polymer functionalization. The functionalization of degradable polymers with amine groups (i.e. NH_2) via aminolyzing reactions is a necessary priming that leads to the crosslinking of other bioactive molecules such as gelatin, chitosan, and collagen.[58] Aminolysis involves treating degradable polyesters such as PCL and PLA with diamine compounds to add amine groups.[24] Essentially, the aminolyzing agents react with the polymer chains by severing the polymer at its ester linkages leading to formation of alcohol and amine functional group.[59] Two popular diamine agents used for aminolysis include ethylenediamine (EDA)[60] and Hexanediamine (HDA).[58, 61] EDA is a very corrosive (MSDA) chemical compound that has been used to directly aminolyze PCL at room temperature.[60] EDA is usually employed as a chemical crosslinker, but analysis shows that PCL treated with EDA alone showed better cellular proliferation when compared to a control PCL sample.[60] Similarly, HDA, a longer diamine chain, has been used to aminolyze both PCL[58] and PLA[61] polymer matrixes. Direct detection methods for the presence of amine groups on degradable polymers include Fourier Transform Infrared Spectroscopy (FT-IR)[57] and Ultra Violet Visible Spectrometry

(UV-Vis).[61] Cell proliferation assays can also be used to determine the effects of added amine functional groups on cellular growth.[62] Although aminolysis is only one of numerous functionalization methods, it is commonly employed as a simple and economic way to perform degradable polymer functionalization.

CHAPTER 3

INTRODUCTION TO RESEARCH

3.1 Significance of Research

The motivation for this research is the development of a novel bionanocomposite hernia mesh that improves the mechanism of wound healing by stimulating better *in vivo* tissue integration, while maintaining adequate mechanical strength during the process. Research performed by Costello et al. (2007) has demonstrated the viability of decellularized porcine diaphragm as a base material for a bionanocomposite hernia mesh.[5] In order to inhibit premature failure of the mesh implant, certain modifications to the decellularized tissue must occur. Modifications such as adding chemical crosslinkers, embedding gold nanoparticles, and electrospinning functionalized degradable polymer nanofibers onto the tissue surface are necessary to both strengthen the bionanocomposite mesh and slow the reabsorption rate of the decellularized tissue.[24]

The research performed in this study specifically addresses the inclusion of electrospun biodegradable polymer nanofibers as a possible synthetic component of the aforementioned bionanocomposite hernia repair mesh. More specifically, the degradable polyester polycaprolactone (PCL) was investigated due to its relative hydrophobicity which allows for a longer degradation time, thus more reliable strength in an integrated bionanocomposite material. Additionally, the relatively low cost of PCL permitted a number of trials to be performed to determine parameters necessary to consistently produce appropriate fiber morphologies. Likewise, aminolysis experiments were carried in an attempt to add amine functional groups to electrospun PCL nanofibers. Amine

functional groups would permit the chemical crosslinking of the PCL fibers to the decellularized porcine diaphragm to produce a more integrated bionanocomposite hernia repair mesh. Appendix 1 provides the protocol for the integration of PCL fibers into the decellularized tissue.

3.2 Outline of Experimental Methods

This research study progressed in three separate phases. The first phase included a dynamic electrospinning parameter study to determine the appropriate experimental conditions to produce PCL polymer nanofibers. The second phase of the study focused on the aminolysis of PCL fibers using the chemical agents ethylenediamine (EDA) and hexanediamine (HDA). The third and final phase addressed a brief comparison study of PCL with a couple other degradable polymers.

Investigating the various experimental parameters associated with electrospinning was accomplished by first constructing an electrospinning apparatus, which was based on a previous design by Sautter et al. (2005) from the University of Illinois at Chicago. The specifics of the electrospinning apparatus are discussed in Chapter 4. However, the basics included a high voltage power source, syringe pump, an adjustable vertical slide, dispensing needle, and grounded plate collector. The experiments of phase 1 included testing the effects of voltage, dispensing needle to ground plate distance, grounded plate orientation, needle diameter, volumetric flow rate, solution concentration, and solvent composition. The only control in the experiments was the use of the polymer PCL in the electrospinning solutions. The resulting fibers were assessed using a compound light

microscope at 400 X resolutions and with Scanning Electron Microscopy (SEM) imaging.

The aminolysis of PCL was investigated. Experiments of phase 2 included two different aminolysis procedures along with two different aminolyzing agents. The first aminolyzing procedure included a "pre-electrospinning" aminolysis of PCL. Essentially, the aminolyzing agent EDA was added to the electrospinning solution before producing the electrospun nanofibers. The other aminolyzing procedure included "post-electrospinning" aminolysis of PCL. This time the EDA or HDA was added to previously electrospun PCL nanofibers to perform the aminolysis. Analysis for this phase was performed using FT-IR to measure the intensity of the amine group absorption peaks. Results for the post-electrospinning mesh aminolysis are posted in Appendix 2.

Phase three experiments included a direct aminolysis comparison study of PCL, PLA and poly (lactide-co-caprolactone) (P(L-co-CL), all of which are degradable polyesters. Experiments tested the effects of applied solution of EDA and HDA to the three polymers. Preliminary results for this experiment are listed in Appendix 3.

CHAPTER 4

ELECTROSPINNING PARAMETERS FOR POLYCAPROLACTONE

4.1 Introduction

The degradable polymer polycaprolactone (PCL) was investigated for its potential use in a novel bionanocomposite hernia mesh material developed by Costello et al. (2007). The first obstacle to tackle in this investigation was the development of reproducible experimental conditions that would support the formation of PCL fibers. As alluded to in the previous chapters, electrospun degradable polymer fibers are believed to mimic a tissue's extracellular matrix, thus promoting tissue growth and integration. In the case of the bionanocomposite mesh, electrospun PCL fibers would be employed to facilitate tissue regeneration, while strengthening the decellularized porcine diaphragm base and inhibiting rapid tissue degeneration once implanted in the body. The ensuing experimentation sought to manipulate the various electrospinning parameters to gain the appropriate knowledge to proceed with the project. Initially, efforts were focused on the formation of electrospun PCL fibers from a preferred control solution. Essentially, a control PCL electrospinning solution with the appropriate external parameters could serve as a base for further polymer modification, such as functionalization.

4.2 The Electrospinning Apparatus

The basic requirements for electrospinning include a suitable solvent to dissolve the polymer, an appropriate solution viscosity and surface tension, an adequate voltage

power supply, and an appropriate electrode separation distance between the dispensing needle and ground plate. While all of these parameters are interdependent, the construction of an electrospinning apparatus was the first priority in this project. Once an integrated apparatus was built, it allowed for the easy manipulation of all of the necessary electrospinning parameters.

Inspiration for the electrospinning apparatus came from a previous design constructed by Sautter et al. (2005) from the University of Illinois at Chicago. The design included a semi-isolated system where the polymer solution, syringe pump, syringe, dispensing needle, ground plate were enclosed in a Plexiglas safety box.[32] External components included a high voltage power supply connected to the dispensing needle and ground plate via electrodes, an AC to DC transformer, and an external CPU interface.[32]

The electrospinning apparatus for this project incorporated many of the ideas from the Sautter et al. (2005) prototype, but certain modifications were implemented in order to make the apparatus more suitable for experimentation. As displayed in Figure 2, a Spellman 230-30R Series Bench-top High Voltage Power Supply (Valhalla, NY) with a maximum voltage output of 30 kV and a 500μA current was used to generate a charge build-up on the polymer solution and create an electric field between the dispensing needle and ground plate. The voltage supply was connected to a (18-22) gauge I&J Fisnar (Fairlawn, NJ), 1.5" blunt-end stainless steel dispensing needle and a 6"x6", 3/32" thick, copper McMaster-Carr (Atlanta, GA) ground plate. Corning, 1"x3" microscope slides were place on the copper ground plate in order to collect electrospun samples for analysis.

A McMaster-Carr ceramic rod 5/8" diameter and 12" long isolated the high voltage needle from the rest of the system as shown in Figure 4. The ceramic rod was attached to an Anaheim Automation LS100 Series slide motor (Anaheim, CA), which had a 15" vertical range. Computer interfacing was outside the scope of this project, so slide motor height adjustments occurred manually. Connection between the dispensing needle and a syringe containing the polymer solution was achieved using Cole-Parmer 1/16" diameter TYGON lab tubing (Vernon Hills, IL). The tubing was attached to both the needle and the syringe using Cole-Parmer male and female l/16" hose barbs. Solution flow rate was controlled with a Braintree Scientific (Braintree, MA) BS-8000 Series syringe pump capable of 0-99 ml/ hr volumetric rates (Figure 3).

As shown in Figure 1, a safety box was constructed in order to isolate the experimental system from the slide motor, syringe pump, and high voltage power supply. The box was 24"x24"x18" in size and was composed of 0.707" thick clear cast acrylic sheets manufactured by McMaster-Carr. A burgundy electrical grade 1/5" fiberglass sheet from McMaster-Carr was used as a contrast backing material for the safety box. As an extra precaution, McMaster-Carr adhesive backed polyester (PET) films were installed within the safety box to dissipate any build-up in electrostatic charges.

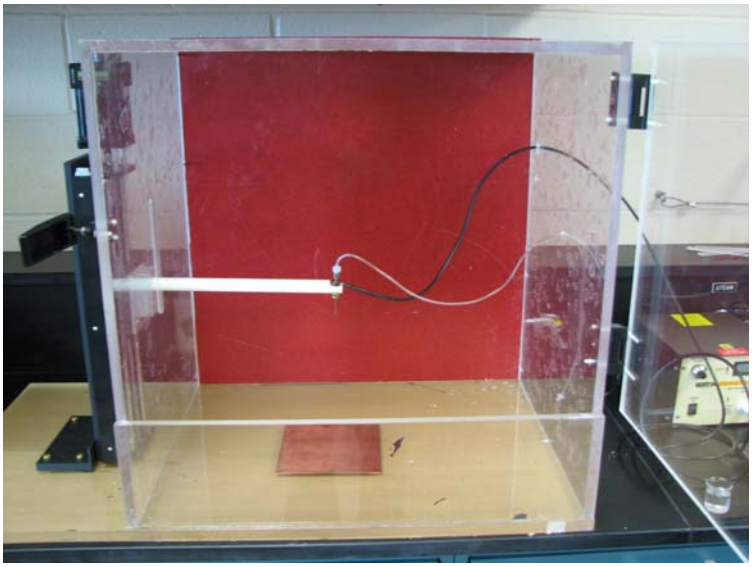

Figure 1: Photograph of the electrospinning apparatus highlighting the safety box, syringe pump and high voltage source component connections, slide motor and copper ground plate

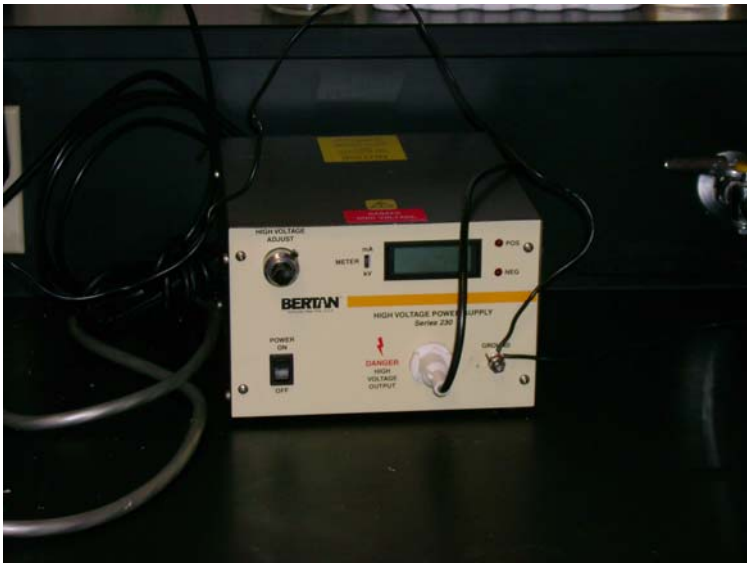

Figure 2: High voltage power supply with attached electrodes

Figure 3: Syringe pump with syringe containing polymer solution attached to TYGON tubing

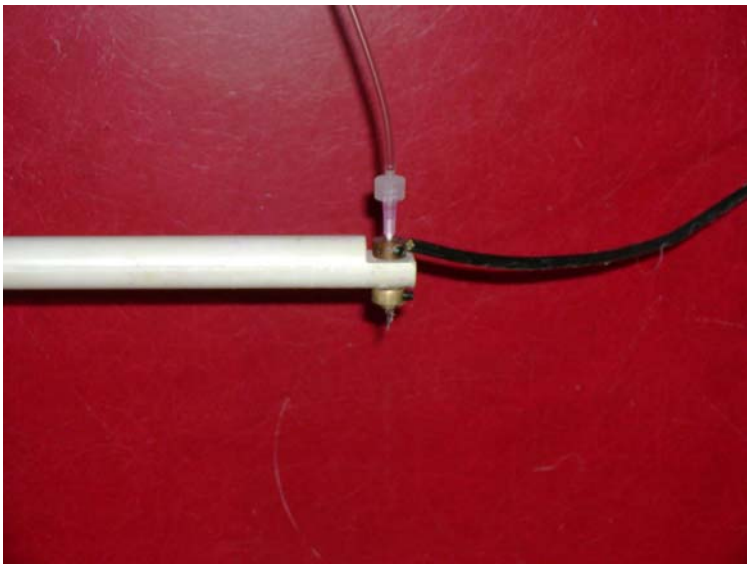

Figure 4: Ceramic rod with dispensing needle connected to TYGON tubing and high voltage power supply electrode

4.3 Materials and Methods

4.3.1 Electrospinning Solution Parameters

Solution viscosity and surface tension dictate a solution's ability to form electrospun polymer fibers. Optimum solution parameters for polymer concentration and

solvent composition vary widely depending on the selected polymer. Polycaprolactone (m.w. = 80,000) from Sigma-Aldrich (St. Louis, MO) was selected for this experimental study. Initial parameters for the PCL solution included a 5% wt/v solution of PCL dissolved in acetone, which was based on prior published results. Experimentally, PCL was prepared in 3-13% wt/v solution concentrations. The solvents used in the solution parameters testing included acetone, toluene, chloroform, and dichloromethane. These solvents were selected for experimentation because they had been previously shown to adequately dissolve PCL at ambient conditions. Once the electrospinning solution components were added together in a test tube, one to three hour sonications coupled with 60-80 C hot water baths were used to thoroughly mix the electrospinning solutions to uniformity. Finally, the prepared solution was cooled to ambient temperature in order to yield a more consistent viscosity and surface tension during the electrospinning process.

4.3.2 The Electrospinning Apparatus Parameters

Once the electrospinning solution formulation is selected, the resulting electrospun fibers are dependent on various parameter manipulations from the electrospinning apparatus. Parameters such as voltage, needle to ground plate separation, syringe pump flow rate, needle gauge, and even ambient conditions can have a dramatic effect on electrospun fiber morphology. Based on published results with PCL electrospinning, initial apparatus parameters were set using a 15 kV voltage, 15 cm plate separation distance, 5 ml/hr flow rate, and 18 gauge dispensing needle. Subsequent experimentation tested and adjusted a variety of electrospinning parameters to determine

the ideal conditions to produce consistently uniform electrospun PCL fibers from a given solution. For instance, the voltage output for the parameter optimization experiments varied between 5 kV and 30 kV. Similarly, experimental syringe pump flow rates ranged from approximately 0.10 ml/ hr to 15 ml/ hr, and the polymer solution dispensing needles varied from 18, 20, and 22 gauge sizes. Needle to ground plate separation distances ranged from 5 cm all the way to 20 cm. Initial testing with these electrospinning apparatus parameters yielded a wealth of knowledge for our lab, which ultimately provided a benchmark for future experiments.

4.3.3 Detection Methods

The series of PCL electrospinning parameter experiments employed the use of a Thermo Scientific compound light microscope and a Scanning Electron Microscope (SEM) to assess the physical morphology of the deposited electrospun fibers. 400x magnification optical zoom digital images from the compound light microscope were taken in order to qualitatively examine the deposited PCL fibers. The qualitative analysis from the digital images provided quick real-time feedback regarding the general morphology of the electrospun fibers. Decisions for experimental adjustments were based on these microscope images. The SEM was used as a secondary tool to provide a more detailed analysis of PCL fiber morphologies. Since SEM analysis could not be provided in real-time, only a few selected samples were examined using this method.

4.4 Experimental Results and Discussion

4.4.1 Solvent Effects

Acetone, toluene, chloroform, and dichloromethane were all tried as potential solvents for a PCL electrospinning solution. While each of the solvents had the ability to dissolve PCL pellets into solution, their performances in the electrospinning application varied greatly.

Acetone (b.p. = 56.53 C) was the first solvent chosen for experimentation. Several experimental test runs revealed that acetone required a three hour solution sonication in ~60 C hot water bath to dissolve the PCL to uniformity in the electrospinning solution. During the electrospinning process PCL/acetone solutions produced uniform electrospun fibers briefly, but needle tip clogging quickly impeded the process after about 30 seconds of electrospinning. It was determined that the low boiling point of acetone resulted in an accelerated evaporation rate, which caused the needle tip clogging. An ideal electrospinning solvent should allow saturated polymer ejection in order to prevent needle clogging, while evaporating before reaching the collection plate. Next, toluene (b.p.= 110.6 C) was tried as a PCL electrospinning solvent due to its much higher boiling point compared to acetone. A preliminary test run, illustrated in Figure 5, however, showed that toluene's evaporation rate was much too slow for an electrospinning application. Subsequently, chloroform (b.p. = 61.2 C) was selected for testing since its boiling point is lower than that of toluene and slightly higher than acetone. The hope was that chloroform's PCL solvent properties would prevent the needle clogging experienced with acetone, but evaporate quick enough to enable a fibrous deposition. Chloroform proved to be much better at dissolving PCL than both

acetone and toluene, evidence by reduced solution sonication times. Additionally, electrospinning PCL/chloroform solutions did not cause needle tip clogging. The downside to chloroform was wet PCL fibrous deposition upon electrospinning, which produced non-uniform PCL fiber morphologies. One last solvent, dichloromethane (b.p. = 40 C), was tested as a PCL electrospinning solvent. Dichloromethane was able to quickly dissolve PCL pellets like chloroform, but the solution solvent evaporation rate occurred even quicker than the PCL/acetone solutions. Needle clogging ensued immediately, thus preventing any fiber deposition.

After numerous experimental tests examining the effects of PCL solvents, it was discovered that a 50% (v/v) electrospinning solution solvent composition of acetone and chloroform was worked the best. The 50% (v/v) acetone to chloroform PCL solution prevented dispensing needle clogging, while evaporating fast enough to enable the formation of relatively uniform PCL fibers when electrospinning. Therefore, all subsequent electrospinning parameter experiments used the 50% (v/v) acetone to chloroform solvent.

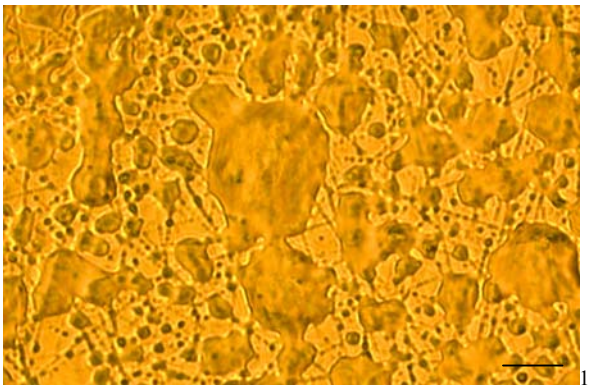

Figure 5: PCL deposition using a pure toluene solvent

4.4.2 Concentration and Needle Gauge Effects

Using the 50% (v/v) acetone to chloroform solvent composition for the PCL electrospinning solution, the effects of PCL concentration were tested. PCL concentrations ranged from 3-13% wt/v during experimentation. During these experiments, needle gauge was tested as well, but it was quickly determined that the 18 gauge needle had a wider range of applicability compared to the 20 and 22 gauge needles. The smaller diameter needles produced smaller solution droplets, thus increasing the surface area to volume ratio. The 20 and 22 gauge needles quickly clogged once the solution was exposed to the air.

A series of experimental test runs with the 18 gauge needle revealed that 8% wt/v PCL electrospinning solution concentration in the 50% (v/v) acetone to chloroform solvent produces the most homogenous fiber deposition. Fiber diameter homogeneity is desired in order to more accurately predict the physical properties of electrospun PCL bulk mesh materials. The test runs shown in Figure 6 suggest that solution concentrations under 8% cause higher bead-to-fiber ratios due to loss of solution viscosity, while concentrations over 8% progress towards larger diameter fibers resulting in more globular sample depositions. Solution concentrations above 10% wt/v hardened at the needle tip due to rapid solvent evaporation.

(a) 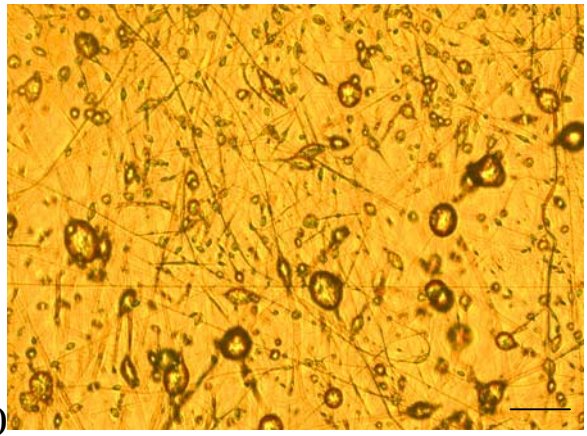 100 µm

(b) 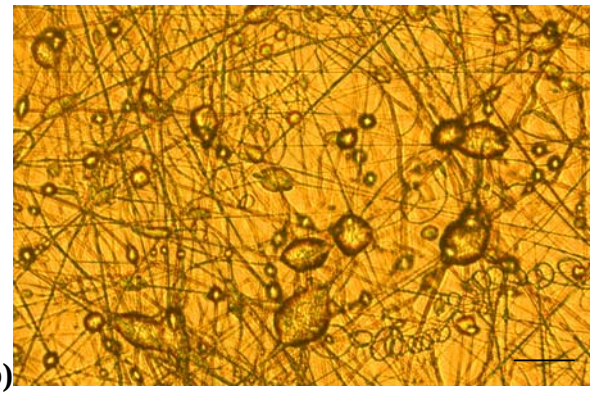 100 µm

(c) 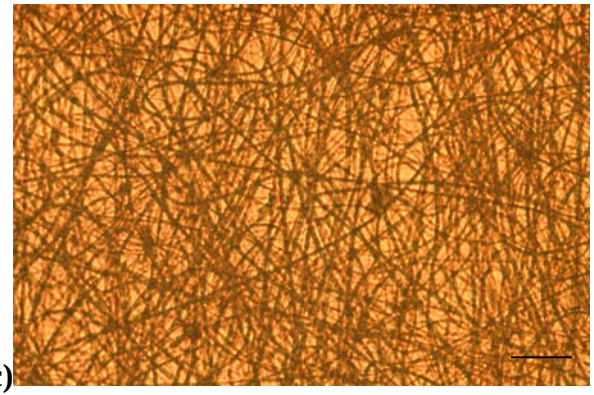 100 µm

(d) 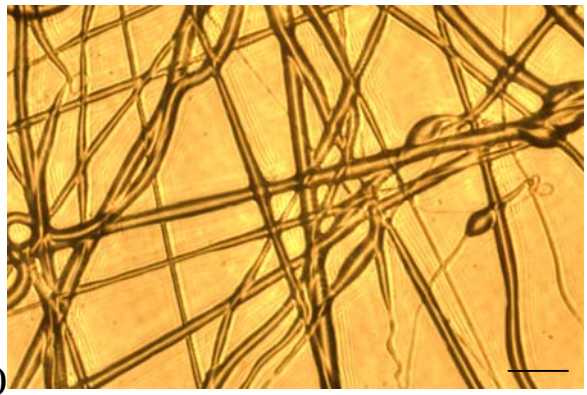

(e) 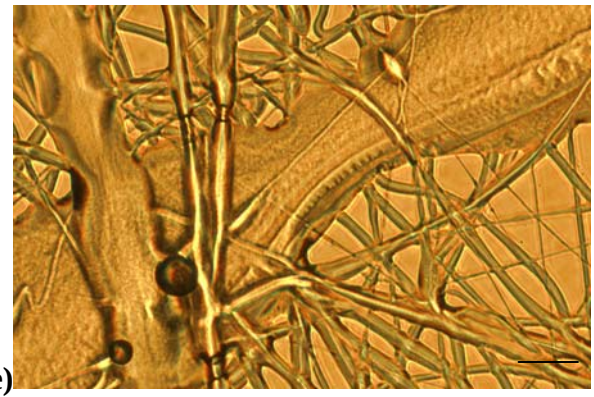

Figure 6: Samples displaying solution concentration effects for PCL electrospinning: (a) 3% wt/v, (b) 5% wt/v, (c) 8% wt/v, (d) 10% wt/v, and (e) 13% wt/v

4.4.3 Flow Rate Effects

As mentioned previously, syringe pump flow rates ranged from 0.10 ml/ hr to 15 ml/ hr during electrospinning apparatus experimentation. All syringe pump flow rate experiments were conducted using the 8% wt/v PCL in 50% (v/v) acetone to chloroform electrospinning solution. Figure 7 illustrates that experimental test runs with the aforementioned solution parameters illustrated that a 3 ml/hr volumetric flow rate would work best. Optimally, the goal of the electrospinning process to allow the formation of an electrospun polymer jet, while replacing the drawn solution at the same rate. Essentially, the needle tip dispenser should constantly provide a bead of solution at the needle tip without clogging or dripping out. Below 3 ml/hr, needle tip solution beads did

not form and the electrospinning solution was drawn off quicker than it was replaced. This resulted in inconsistent electrospinning and needle clogging, and rates below 1 ml/hr did not produce any electrospun product at all. Flow rates higher than 3 ml/hr caused the solution to begin to drip from the needle tip, which caused a globular sample deposition with larger diameter fibers. Above 10 ml/hr recognizable PCL fibrous deposition does not occur.

(a) 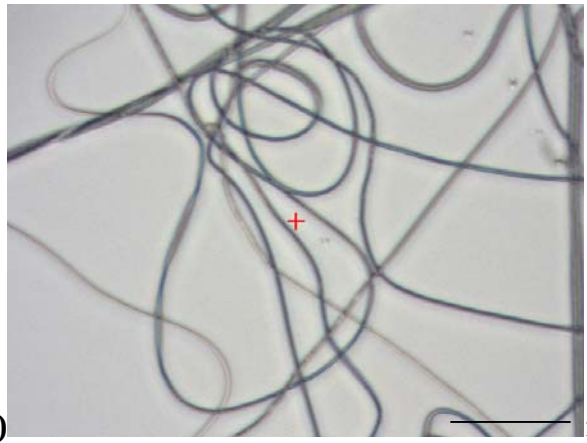

(b) 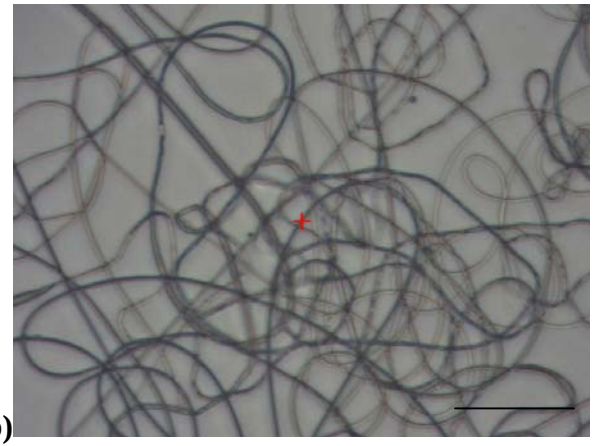

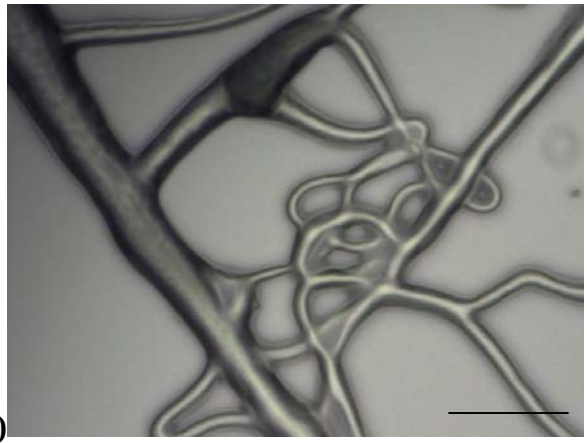

Figure 7: Samples displaying solution flow rate effects for PCL electrospinning: (a) 1 ml/ hr, (b) 3 ml/ hr, (c) 6 ml/ hr, and (d) 10 ml/ hr

4.4.4 Voltage Effects

Experimental voltage effect analysis was performed for the PCL electrospinning solution using an output voltage range between 5 kV and 30 kV. In order to build off of previous experimental results, the voltage effect experiments used the 8% wt/v PCL in 50% (v/v) acetone to chloroform electrospinning solution at a 3 ml/ hr flow rate. Figure 8 suggests that a 21 kV potential allowed for the best results. Voltages below 7 kV did not permit electrospinning jet formations, resulting in no fiber deposition. Between 7 and 21 kV fiber deposition was interrupted with globular deposits since polymer jet ejection

did not keep up with solution formation at the needle tip. Conversely, voltage potentials above 21 kV caused polymer jet ejection to occur at a higher rate than solution formation at the needle tip. This resulted in intermittent fiber deposition and eventual needle clogging due to rapid solvent evaporation at the needle tip.

(a) 

(b) 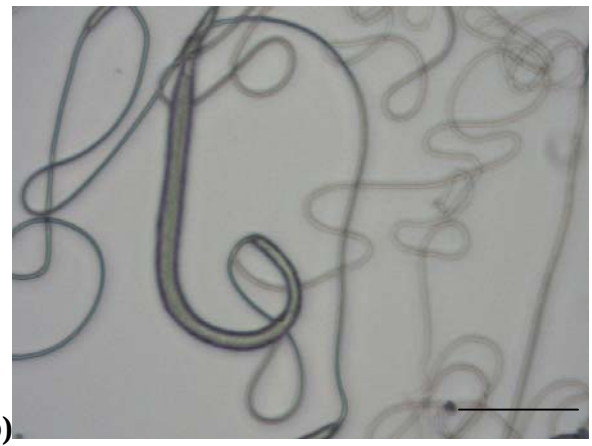

(c) 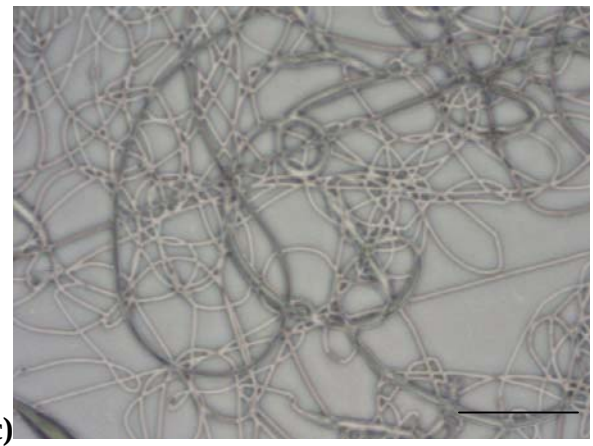

(d) 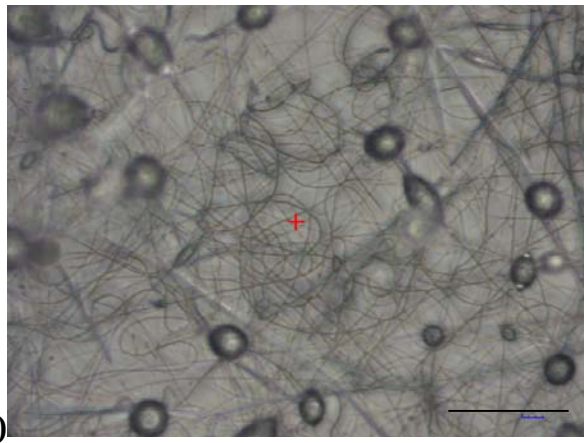

Figure 8: Samples displaying solution voltage effects for PCL electrospinning: (a) 10 kV, (b) 15 kV, (c) 21 kV, and (d) 27 kV

4.4.5 Plate Separation Effects

The final set of parameter adjustment experiments tested the effects of vertical plate separation between 5 cm and 20 cm. Twenty centimeters was the maximum allowed separation distance due to safety constraints. It was feared that plate separations exceeding 20 cm might result in the charged electrospun polymer stream to arc back into the conductive slide motor adjustment arm. The control electrospinning parameters for these experiments included 8% w/v PCL in 50% (v/v) acetone to chloroform with a 3ml/ hr flow rate and a 21 kV voltage potential. As with the voltage adjustment test runs, the plate separation tests affected both the charge build-up on the polymer solution and the strength of the electric field. It was determined that the original baseline separation distance of 15 cm between the needle tip and copper collection plate produces the most consistent results. Essentially, plate separation distance is inversely related to voltage supply. Plate separation distances in excess of 15 cm produced inconsistent large diameter globular fibers; whereas, separation distances under 15 cm caused intermittent fiber depositions due to the solution being extracted too quickly.

4.5 Conclusion

Although the parameter tests were extremely exhaustive, they provided exceptional insight regarding the complex process of electrospinning. The preliminary polycaprolactone electrospinning tests allowed the development of a solid set of parameters for electrospinning PCL. Both the electrospinning solution composition and electrospinning apparatus parameters derived from these preliminary experiments provided the basis for all subsequent experiments in the bionanocomposite study.

From the data gathered, it was determined that an 8% wt/v PCL in 50% (v/v) acetone to chloroform would produce optimum fiber deposition when electrospun with an 18 gauge needle, 15 cm vertical plate separation, 21 kV potential, and 3.0 ml/hr flow rate. These parameters produced consistent results in multiple experimental test runs. The SEM images in Figure 9 and Figure 10 show uniformity in the electrospun fiber structure as well sub-micron fiber diameters. This latter quality is crucial if the electrospun product is to be incorporated into a bionanocomposite material.

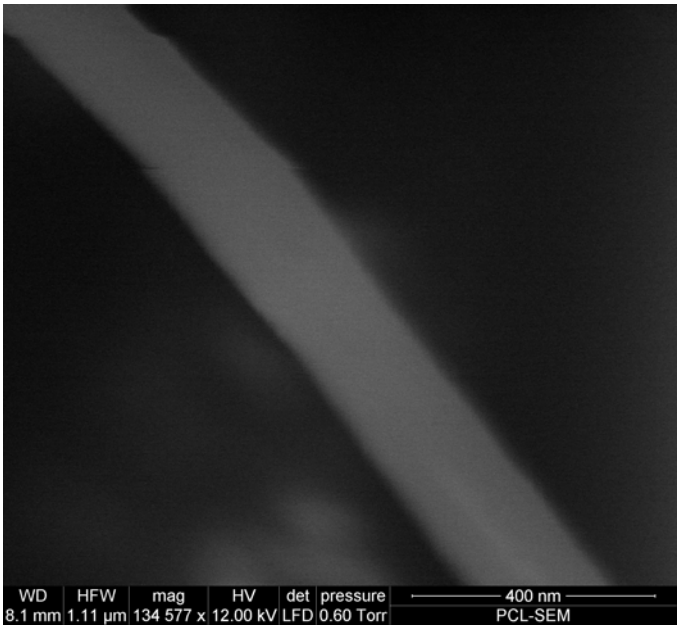

Figure 9: SEM of single electrospun PCL fiber

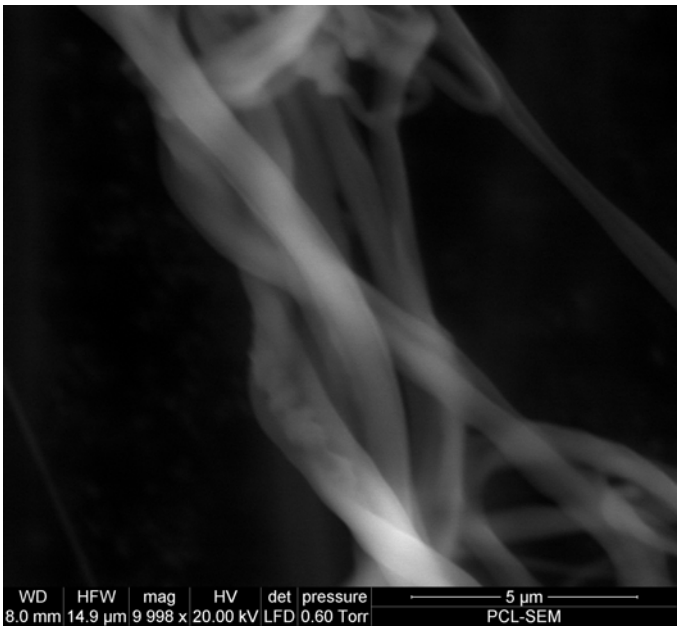

Figure 10: SEM of electrospun PCL fiber grouping

CHAPTER 5

PCL AMINOLYSIS PROTOCOLS

5.1 Introduction

The goal of the PCL aminolysis experiments was to develop a successful protocol to perform amine group functionalization of electrospun PCL fibers. As mentioned previously in the literature review, the amine group functionalization of PCL permits the electrospun PCL fibers to chemically crosslink with various components of a tissue engineered bio-scaffold. Essentially, the scope of this project necessitates the functionalization of electrospun PCL fibers with amine groups in order to form chemical crosslinks to the carboxyl groups of the porcine diaphragm tissue

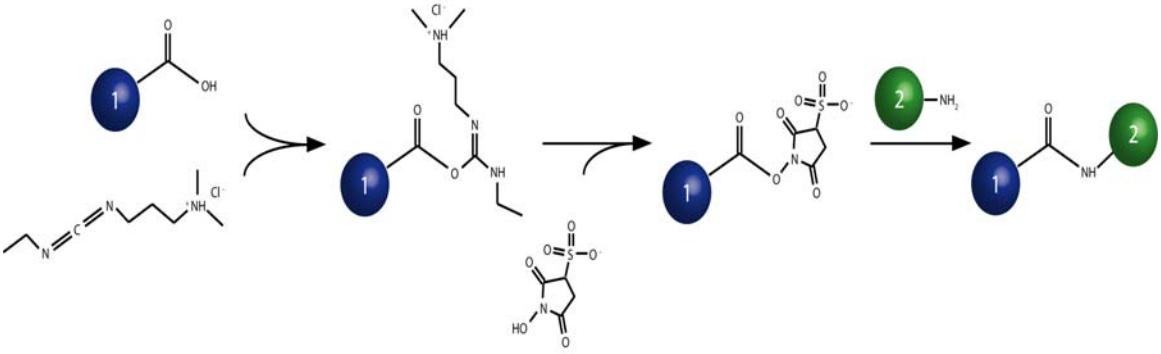

Figure 11: Crosslinking of amine-functionalized PCL fibers to decellularized porcine diaphragm ("1"= decellularized diaphragm; "2"= functionalized PCL fiber)
***Graphic provided by R. Cody Stringer, University of Missouri**

The method of aminolysis was chosen for the amine group functionalization of PCL for a couple of reasons. The first reason was due to its procedural simplicity as there are relatively few steps to perform in PCL aminolysis. The second reason was the low cost of materials and equipment compared to other functionalization methods. Three different

PCL aminolysis protocols were attempted in this project and are outlined in the next section.

It should be noted that the focus of the aminolysis experiments was not the optimization of the electrospun fiber morphologies. Baseline electrospinning parameters were put forth for the aminolysis experimental test runs, but due to project time constraints, these parameters were often altered to obtain fiber deposition in order to perform analysis. The decision to alter electrospinning parameters during the experiments was justified by the need to develop a working aminolysis protocol that produced amine functionalized PCL fibers. Electrospinning parameters could always be optimized at later time to accommodate specific fiber morphologies.

5.2 Materials and Methods

5.2.1 Initial 2-Step Electrospinning Solution Aminolysis

The initial 2-step electrospinning solution aminolysis protocol is based on a protocol published by Gabriel et al. (2006), which provides a protocol to perform aminolysis on PCL films. According to the paper, optimal aminolysis is performed by soaking PCL films in an aminolyzing solution consisting of 40% (v/v) ethylene diamine in distilled water. The films are incubated in the solution overnight at room temperature, and then washed in DI water for 2 hours.[60] The protocol by Gabriel et al. (2006) was modified in order to perform aminolysis on PCL before the electrospinning process with the aim of electrospinning PCL fibers with amine functional groups already attached. This process would be beneficial since it eliminates the need to chemically treat the PCL fibers after electrospinning, thus preventing any morphological changes to the

electrospun fibers. Essentially, the electrospun PCL fibers would retain their physical properties upon formation, instead of losing strength and structural integrity from a post-electrospinning chemical treatment.

The 2-step electrospinning solution aminolysis required two separate processes to form the final electrospinning solution. Essentially, an 8% wt/v PCL solution was prepared in an aminolyzing solvent consisting of a volumetric ratio of 40% EDA, 30% acetone, and 30% chloroform. The solution was then sonicated for two hours in a 60 C hot water bath. At this point, the solution was either allowed to incubate at room temperature for up to 24 more hours or was immediately centrifuged and decanted to obtain the aminolysed PCL precipitate. (If incubation was chosen, the solution was centrifuged and decanted after the prescribed incubation time.) The aminolyzed PCL precipitate was next washed with ddH2O on an orbital shaker for two hours before being air-dried and weighed. The weighed aminolysed PCL precipitate was then re-dissolved in 50% (v/v) acetone to chloroform to reconstitute an 8% wt/v electrospinning solution. Later experimental runs used a chloroform solution to re-dissolve the aminolysed PCL precipitate for the electrospinning solution. The aminolysed PCL solutions were compared against themselves as well as a control PCL solution consisting of 8% wt/v PCL dissolved in 50% (v/v) acetone to chloroform. (The control solution underwent the same two hour sonication in an 80 C hot water bath before electrospinning).

The baseline electrospinning parameters included an 18 gauge stainless steel blunt-end dispensing needle, a copper ground plate, 15 centimeter vertical needle to ground plate electrode separation, 21 kV potential, 3 ml/ hr flow rate, 1"x3" inch glass slide for sample collection, and ~1 ml total solution deposition per sample. The solution

flow rate was manually controlled by hand, and the electrode spacing and voltages were often altered during the experiment in order to obtain a fiber deposition for FT-IR analysis.

5.2.2 1-Step Electrospinning Solution Aminolysis

The 1-step electrospinning solution aminolysis was developed with the goal of producing a PCL aminolysis solution that could be directly electrospun. Essentially, this new method modified the 2-step aminolysis protocol by replacing the 50% (v/v) acetone to chloroform solvent with pure chloroform in the aminolyzing solution in order to eliminate the formation of a solid aminolysed PCL precipitate. More importantly, a direct 1-step aminolysed electrospinning solution would have more standardized solution properties, thus inhibiting the inconsistencies experienced in the 2-step method when dissolving the aminolysed PCL precipitate.

The 1-step aminolyzing solution consisted of 10% wt/v PCL dissolved in 20-40% (v/v) EDA to chloroform. The 10% wt/v solution replaced the 8% wt/v solution because it was found that aminolysis significantly reduces solution viscosity, therefore necessitating a more viscous initial solution concentration in order to form electrospun fibers. The control solution consisted of 8% wt/v PCL dissolved in 50 % (v/v) acetone to chloroform. All electrospinning solutions underwent two hour sonications at 80 C before being electrospun. The 1-step aminolysis method did not include incubation after initial sonication. It was determined during the initial 2-step aminolysis tests that extensive loss of solution viscosity accompanies extended incubations of the aminolyzing solutions.

Decellularized porcine diaphragm tendon was utilized in a test study application of the 1-step electrospinning solution aminolysis protocol. A detailed protocol for this study is provided in Appendix 1. Essentially, the study used the 1-step aminolysis electrospinning solution to directly electrospin onto five decellularized porcine diaphragm samples. The goal of the study was to determine if amine-functionalized PCL fibrous films would chemically or physically attach to the decellularized tissue scaffolds. FT-IR solution and mesh analysis along with qualitative observation were utilized in the assessment of this study.

The baseline electrospinning parameters outlined in the 2-step aminolysis protocol were utilized in 1-step electrospinning solution aminolysis as well. As in the 2-step aminolysis experiments, manually controlled solution flow rates, variable electrode separation distances, and variable voltages were applied during the electrospinning process in attempt to form fibrous samples for FT-IR analysis.

5.2.3 Electrospun Mesh Aminolysis

The electrospun mesh aminolysis protocols were carried out as a retrograde comparison to the 1-step and 2-step electrospinning solution aminolysis protocols. Essentially, the electrospun mesh aminolysis protocols directly tested the effectiveness of the PCL aminolysis protocols from the Gabriel et al. (2006) and the Zhu et al. (2002) papers. Although both papers utilized PCL films in their respective aminolyzing procedures, electrospun PCL meshes were used here instead. The electrospun meshes were produced from a control solution consisting of 8% wt/v PCL in 50% (v/v) acetone to chloroform. The electrospinning parameters used in both the 2-step and 1-step

aminolysis experiments were implemented here and were unchanged as well. However, unlike the 2-step and 1-step aminolysis solution experiments, the electrospinning parameters were kept constant during the course of the test runs. Each deposited electrospun mesh was produced from ~1 ml of electrospinning solution.

The first electrospun mesh aminolysis protocol was similar to the Gabriel et al. (2006) paper. Electrospun PCL meshes were placed in variable aminolyzing solution consisting of 0-100% (v/v) EDA in distilled water. The meshes were then incubated at room temperature for 24 hours, and then washed with distilled water on an orbital shaker for two hours before further analysis.

The second electrospun mesh aminolysis protocol was based on the Zhu et al. paper (2002) for aminolysis with HDA. The PCL meshes were incubated for one hour in a solution consisting of 10% wt HDA in isopropyl alcohol. After incubation, the treated meshes were washed with distilled water for 2 hours on the orbital shaker before further analysis

5.2.4 Detection Methods

The analysis conducted for the PCL aminolysis primarily focused on the use of FT-IR to determine the presence of amine functional group peaks. Figure 12 depicts the two discernable peak ranges for both the 1-step and 2-step aminolysis methods that differed from the control samples. One peak occurred in the 3201-3423 cm^{-1} range (peak 1). The other peak occurred in the 1508-1660 cm^{-1} range (peak 2). The degree of amine group functionalization was quantitatively measured as the area under each peak.

FT-IR analysis for the 1-step and 2-step solution aminolysis methods was conducted in a similar fashion. A FT-IR scan of a washed drop-cast sample of the electrospinning solution was taken initially. Then, a final FT-IR scan was taken of the washed electrospun sample. All FT-IR samples were washed in ddH2O for two hours and allowed to air dry prior to a FT-IR scan. The mesh aminolysis samples were similarly analyzed with FT-IR, only without initial electrospinning solution scans.

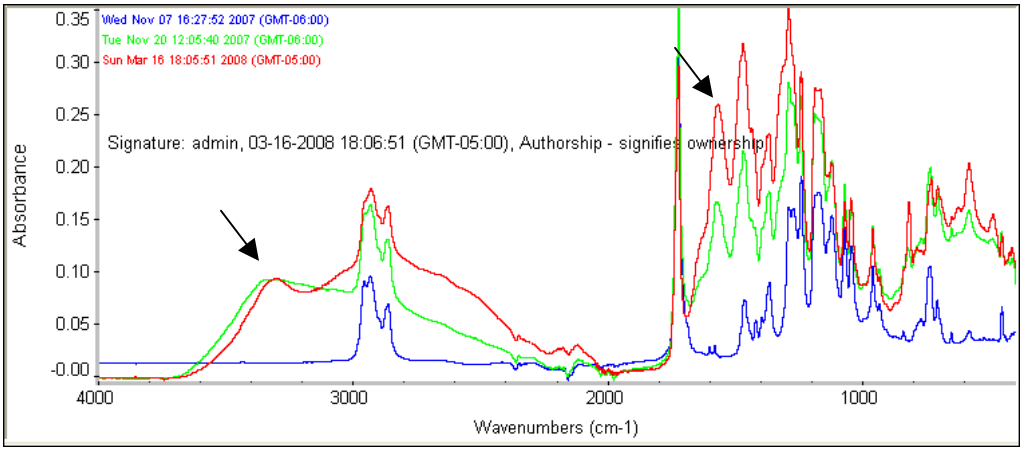

Figure 12: FT-IR data graph for control (blue), 2-step aminolysis (green), and 1-step aminolysis (red) electrospun meshes depicting the location of tested peaks

5.3 Experimental Results and Discussion

5.3.1 Analysis of FT-IR Peak Wavenumbers

A graphical FT-IR peak wavenumber (cm^{-1}) comparison for 2-step and 1-step aminolysis samples is presented in Figure 13. The graphs represent the two peaks that fell in the 3201-3423 cm^{-1} (peak 1) and 1508-1660 cm^{-1} (peak 2) range, respectively. The first four graphs (a-d) show 2-step to 1-step aminolysis peak wavenumber analysis, comparing pre-electrospun solutions and electrospun meshes separately. The other four graphs (e-h) provide a wavenumber pre-electrospun solution to electrospun mesh

comparison for each aminolysis method individually. Control samples are not presented due to the absence of wavenumber peaks in two ranges provided above.

Unpaired, two-tailed t-tests were performed on the data sets from Figure 13, and are listed in Table 1. The results show no statistical significance ($p<0.05$) for any of the analyzed data sets. The hypothesis of peak shifting as a result of variation in sample type or the aminolysis treatment method is disproved. Statistically, the selected FT-IR wavenumber peaks in occur in the same region. Therefore, the wavenumber peak ranges of 3201-3423 $^{cm-1}$ and 1508-1660 cm^{-1} for peak 1 and peak 2, respectively, were justified for further use in the FT-IR peak area analysis studies to determine the degree of amine-group functionalization of PCL.

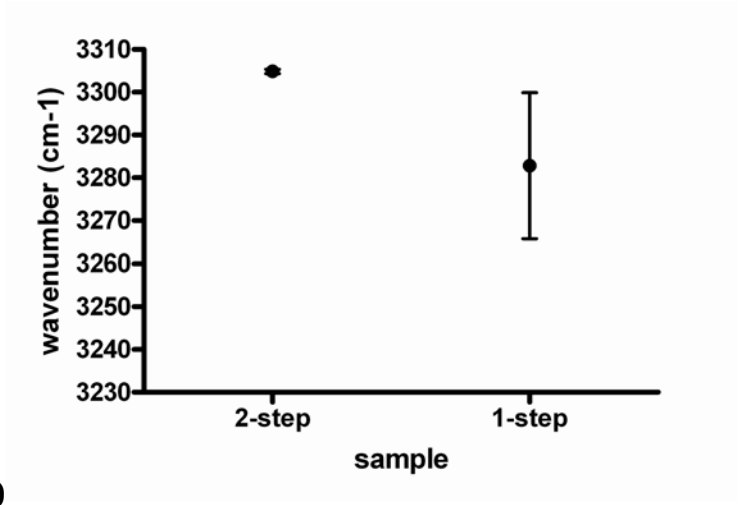

(a)

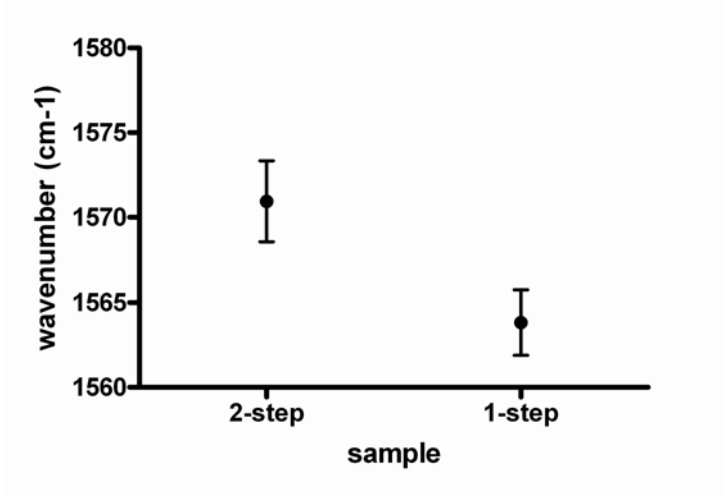
1580
1575
1570
1565
1560
wavenumber (cm-1)
2-step
1-step
sample

(b)

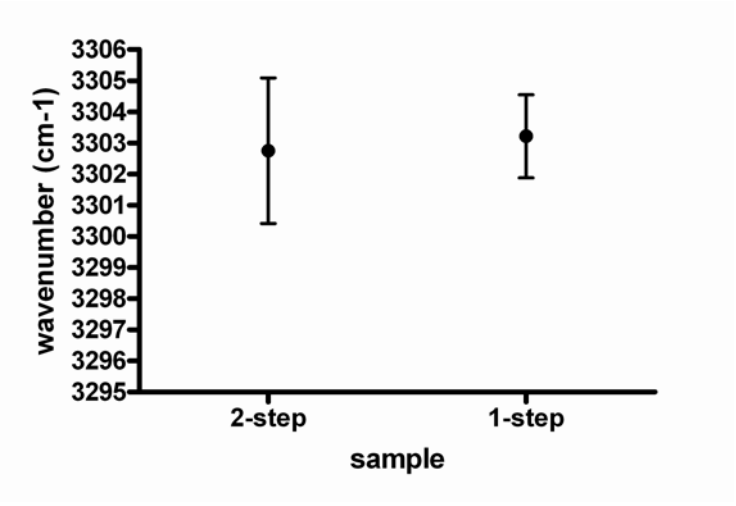
3306
3305
3304
3303
3302
3301
3300
3299
3298
3297
3296
3295
wavenumber (cm-1)
2-step
1-step
sample

(c)

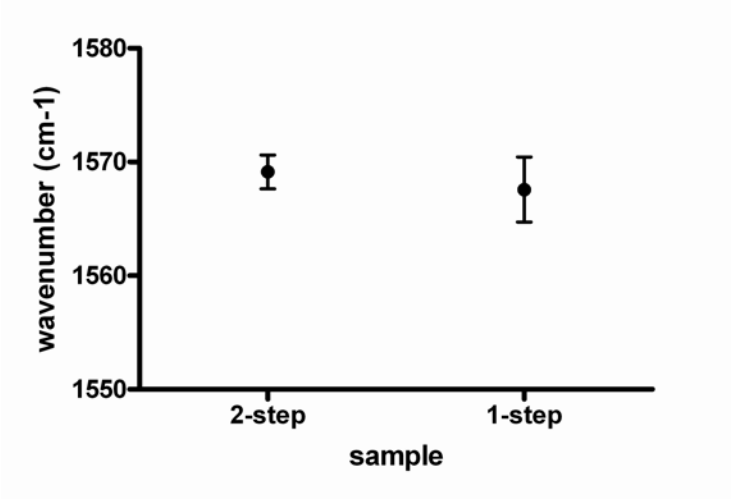
1580
1570
1560
1550
wavenumber (cm-1)
2-step
1-step
sample

(d)

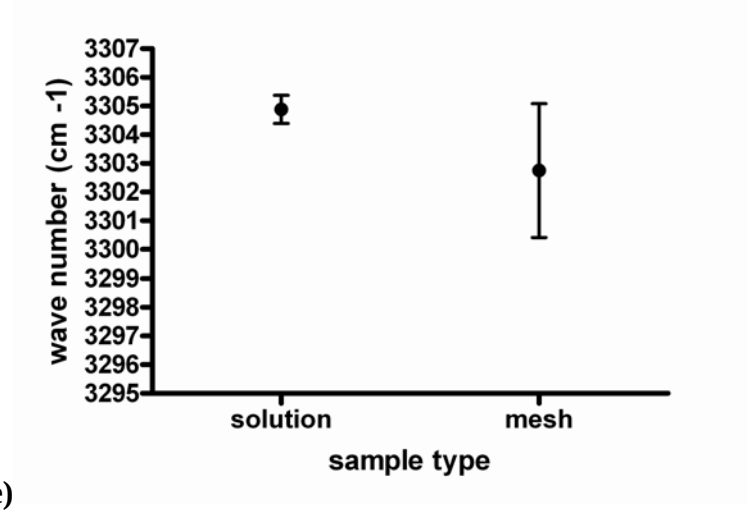
wave number (cm -1)
3307
3306
3305
3304
3303
3302
3301
3300
3299
3298
3297
3296
3295
solution
mesh
sample type

(e)

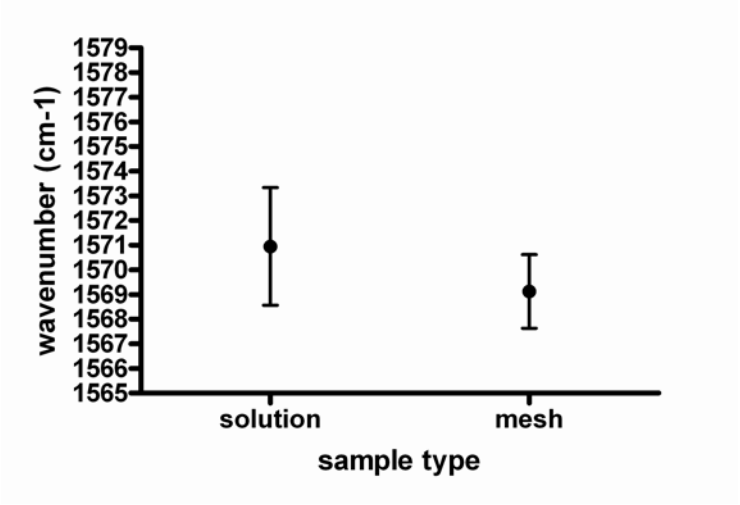
wavenumber (cm-1)
1579
1578
1577
1576
1575
1574
1573
1572
1571
1570
1569
1568
1567
1566
1565
solution
mesh
sample type

(f)

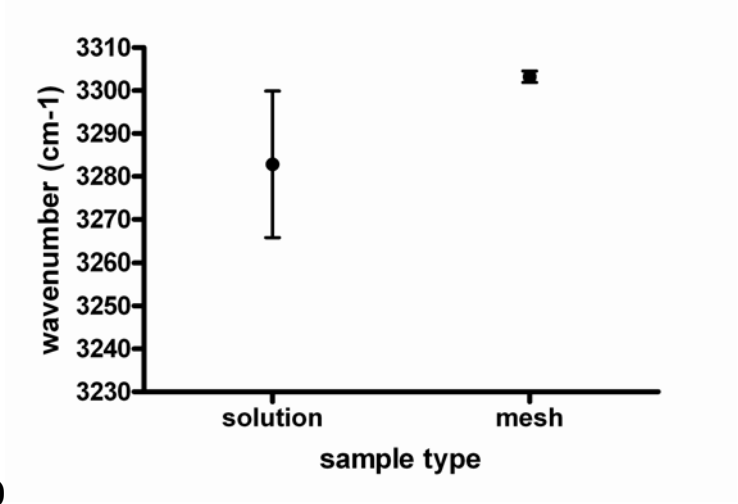

(g)

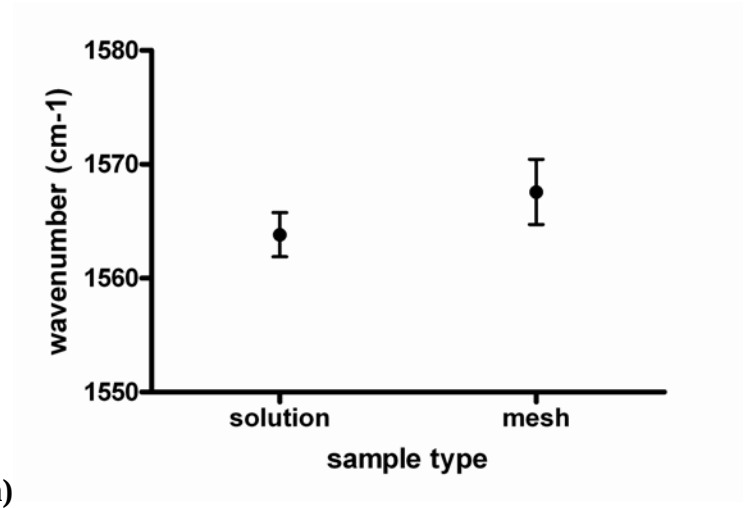

(h)

Figure 13: FT-IR peak wave numbers for (a) 2-step to 1-step peak 1 solution comparison, (b) 2-step to 1-step peak 2 solution comparison, (c) 2-step to 1-step peak 1 mesh comparison, (d) 2-step to 1-step peak 2 mesh comparison, (e) 2-step solution to mesh peak 1 comparison, (f) 2-step solution to mesh peak 2 comparison, (g) 1-step solution to mesh peak 1 comparison, (h) 1-step solution to mesh peak 2 comparison

Table 1: Unpaired two-tailed t-test p-values and sample peak wavenumber means for Figure 3. (P-values <0.05 are significant)

Test Group	Mean P-value	Sample 1 Mean	Sample 2 Mean
2-step to 1-step peak 1 solution comparison	0.1413	3305 ± 0.4875 N=6	3283 ± 17.08 N=4
2-step to 1-step peak 2 solution comparison	0.0666	1571 ± 2.390 N=6	1564 ± 1.938 N=4
2-step to 1-step peak 1 mesh comparison	0.8559	3303 ± 2.340 N=4	3303 ± 1.333 N=6
2-step to 1-step peak 2 mesh comparison	0.6899	1569 ± 1.497 N=4	1568 ± 2.860 N=6
2-step solution to mesh peak 1 comparison	0.3052	3305 ± 0.4875 N=6	3303 ± 2.340 N=4
2-step solution to mesh peak 2 comparison	0.5857	1571 ± 2.390 N=6	1569 ± 1.497 N=4
1-step solution to mesh peak 1 comparison	0.1722	3283 ± 17.08 N=4	3303 ± 1.333 N=6
-step solution to mesh peak 2 comparison	0.3642	1564 ± 1.938 N=4	1568 ± 2.860 N=6

5.3.2 2-Step Aminolysis FT-IR Peak Area Analysis

FT-IR peak range area comparison for the 2-step aminolysis samples is presented in Figure 14. The graphs represent sample peak range areas that fell in the 3201-3423 cm^{-1} and 1508-1660 cm^{-1} range, respectively. The first four graphs show control sample to 2-step aminolysis peak area analysis, comparing pre-electrospun solutions and electrospun meshes separately. The latter two graphs provide a peak range area comparison between solution and mesh samples for the 2-step aminolysis method.

Table 2 lists the statistical analysis for the Figure 14 data sets. Each data set underwent an unpaired, two-tailed t-test to test for statistical differences between the wavenumber peak areas. The results show that there is statistical wavenumber peak area difference ($p<0.05$) between the 2-step aminolysis treatment groups and the control groups, with the exception of the data sets from Figure 14a (control to 2-step peak 1 area solution comparison). However, this outlier can most likely be attributed to the small number of samples in the data set. Within the 2-step aminolysis treatment group there was no statistical significance in peak area between the pre-electrospun solution samples and electrospun mesh samples. This is important because it suggests that the degree of amine-group functionalization from the pre-electrospun solutions is not lost upon formation of the electrospun mesh products.

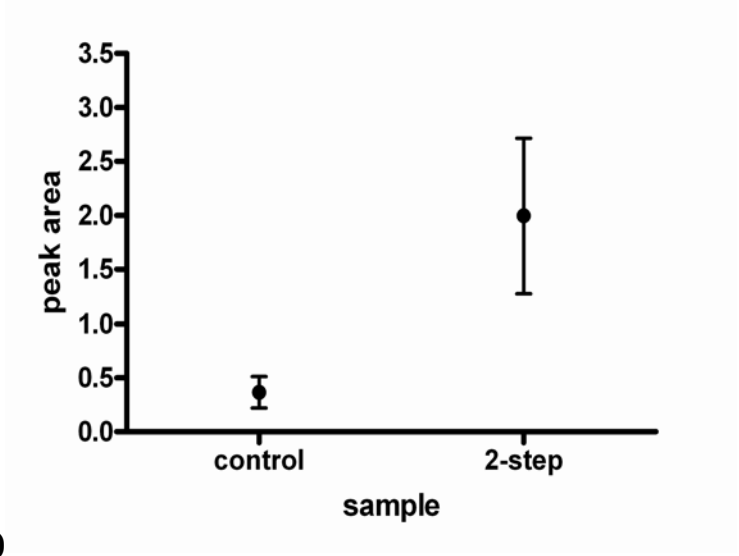

(a)

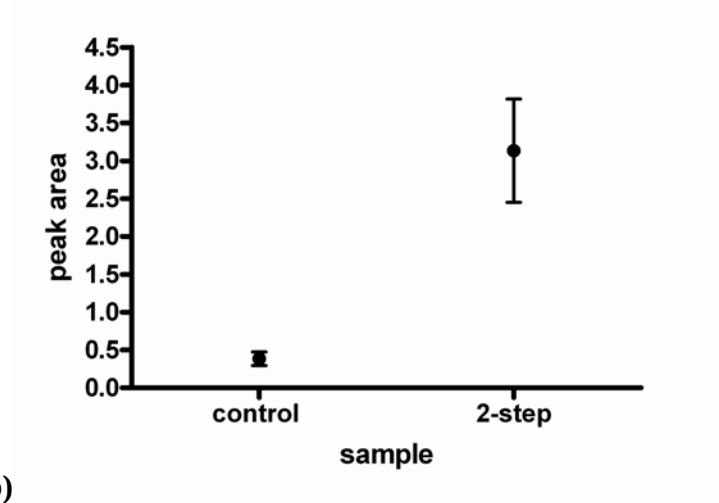
4.5
4.0
3.5
3.0
2.5
2.0
1.5
1.0
0.5
0.0
peak area
control
2-step
sample

(b)

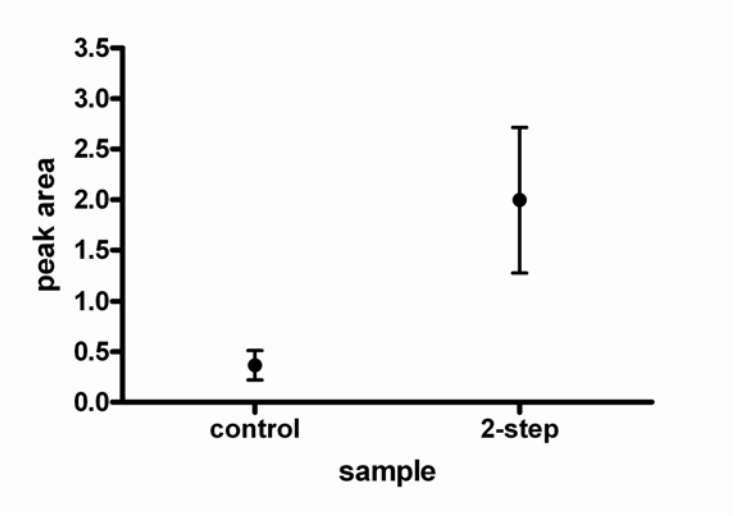
3.5
3.0
2.5
2.0
1.5
1.0
0.5
0.0
peak area
control
2-step
sample

(c)

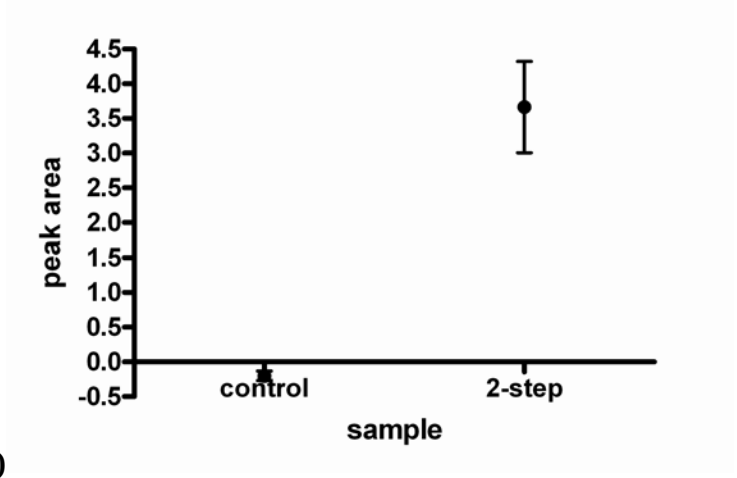
4.5
4.0
3.5
3.0
2.5
2.0
1.5
1.0
0.5
0.0
-0.5
peak area
control
2-step
sample

(d)

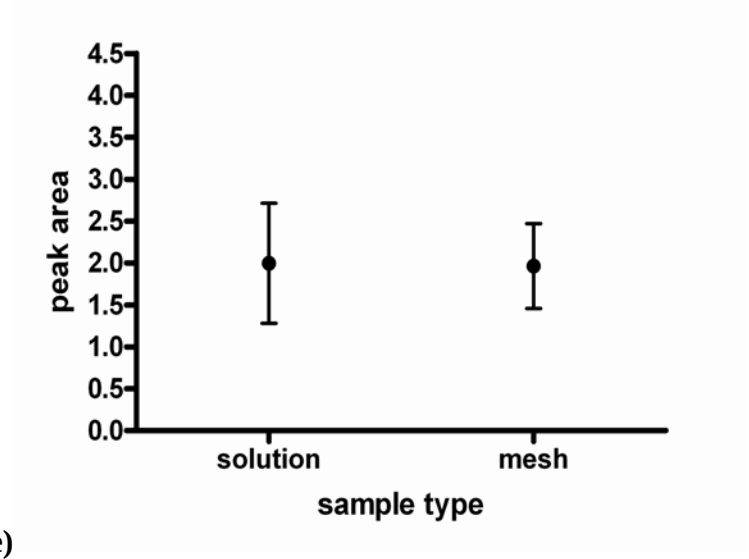

(e)

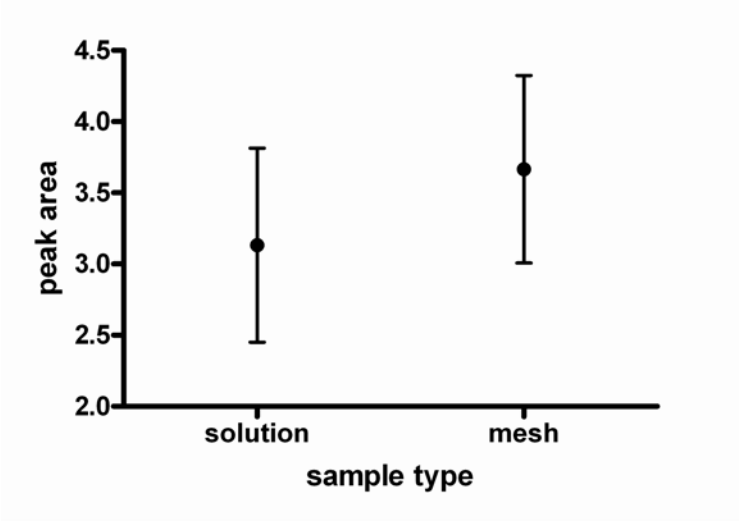

(f)

Figure 14: 2-step aminolysis peak areas for (a) control to 2-step peak 1 area solution comparison, (b) control to 2-step peak 2 area solution comparison, (c) control to 2-step peak 1 area mesh comparison, (d) control to 2-step peak 2 area mesh comparison, (e) 2-step solution to mesh peak 1 area comparison, (f) 2-step solution to mesh peak 2 area comparison

Table 2: Unpaired two-tailed t-test p-values and sample peak areas for Figure 14. (P-values <0.05 are significant)

Test Group	Mean P-value	Sample 1 Peak Area	Sample 2 Peak Area
control to 2-step peak 1 area solution comparison	0.1788	0.3658 ± 0.1458 N=2	1.997 ± 0.7177 N=3
control to 2-step peak 2 area solution comparison	0.0527	0.3830 ± 0.09000 N=2	3.132 ± 0.6819 N=3
control to 2-step peak 1 area mesh comparison	0.0145	0.03133 ± 0.01122 N=3	1.964 ± 0.5070 N=2
control to 2-step peak 2 area mesh comparison	0.0044	-0.2010 ± 0.06906 N=3	3.666 ± 0.6575 N=2
2-step solution to mesh peak 1 area comparison	0.9760	1.997 ± 0.7177 N=3	1.964 ± 0.5070 N=2
2-step solution to mesh peak 2 area comparison	0.6333	3.132 ± 0.6819 N=3	3.666 ± 0.6575 N=2

5.3.3 2-Step FT-IR Peak Area Analysis with Incubation Time

Figure 15 addresses the effect of 2-step aminolysis solution incubation on FT-IR peak range areas. Essentially, the same analysis performed for the non-incubated 2-step samples was performed here. However, no statistical analysis of peak area variance could be conducted between test groups due to the lack of samples (only one incubation test was performed).

The experimental test runs yielded unfavorable results for aminolysis solution incubation. Accordingly, prolonged 2-step aminolysis incubation was abandoned in further tests and was deemed ineffective for the purpose of the project. The decision was

based on the large loss of solution viscosity that accompanied prolonged incubation times, which inhibited the formation of electrospun fibrous meshes. The 24 hour incubation solution sample did not permit the formation of electrospun meshes at all, resulting in the absence FT-IR mesh data. Similarly, the 8 hour incubation formed very few fibers upon electrospinning.

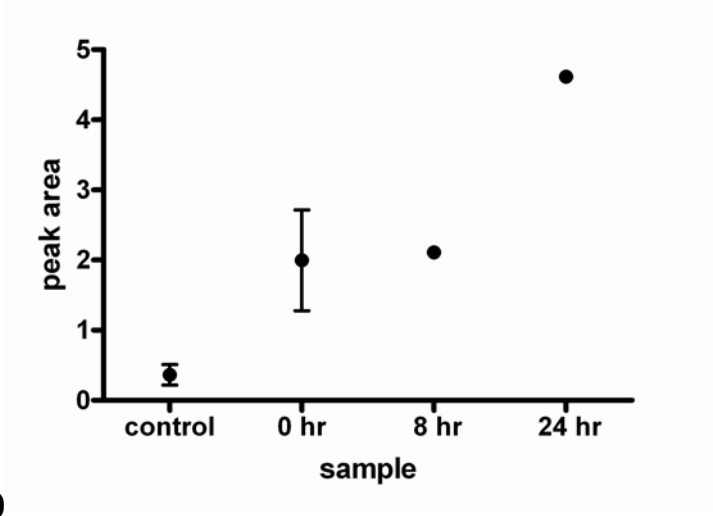

(a)

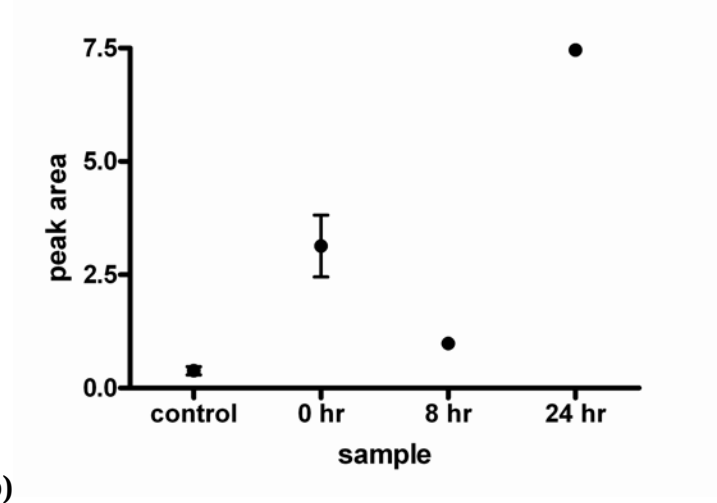

(b)

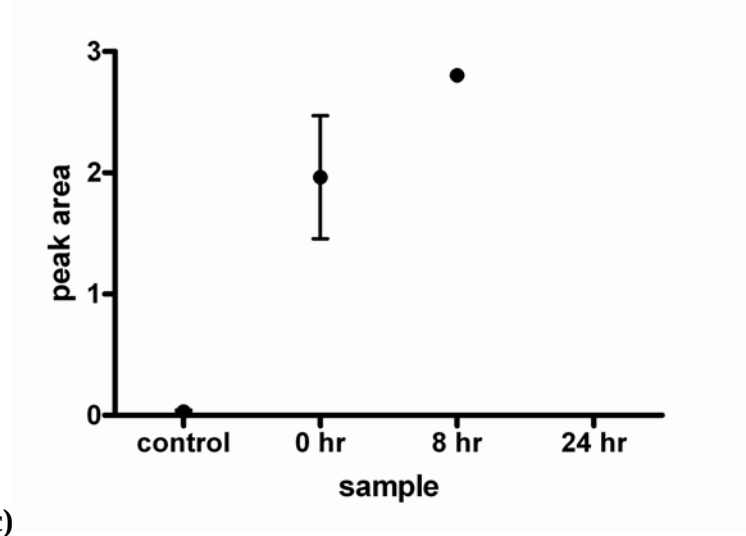

(c)

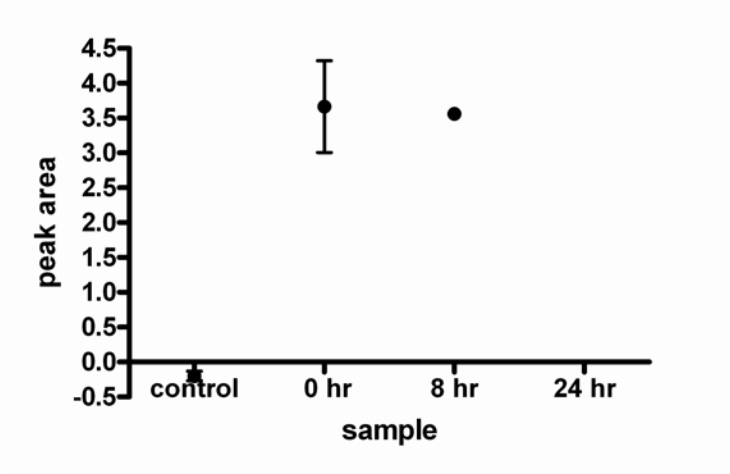

(d)

Figure 15: 2-step aminolysis incubation analysis of peak areas for (a) control vs. 2-step peak 1 area solution incubation times, (b) control vs. 2-step peak 2 area solution incubation times, (c) control vs. 2-step peak 1 area mesh incubation times, (d) control vs. 2-step peak 2 area mesh incubation times

5.3.4 1-Step Aminolysis FT-IR Peak Area Analysis

Similar to the 2-step FT-IR peak range area comparison, analysis for the 1-step aminolysis samples is presented in Figure 16. The graphs represent sample peak range areas that fell in the 3201-3423 cm^{-1} and 1508-1660 cm^{-1} range, respectively. The first four graphs show control sample to 1-step aminolysis peak area analysis, comparing pre-electrospun solutions and electrospun meshes separately. The latter two graphs provide a

peak range area comparison between solution and mesh samples for the 1-step aminolysis method.

Statistical analysis for the Figure 16 data sets for the control to 1-step aminolysis comparisons are listed in Table 3. Once again, unpaired, two-tailed t-tests were conducted to determine whether or not statistical differences existed among the wavenumber peak range areas. The results show that there is statistical wavenumber peak area difference ($p<0.05$) between the 1-step aminolysis treatment groups and the control groups for the electrospun mesh comparisons. The pre-electrospun solutions for the 1-step treatment group were not found to be significantly different for either peak area range when compared to the control solutions. Graphically the peak area means for the 1-step solutions appear higher, but due to the lack of samples and large intra-treatment peak area variances, the comparison was not significantly different. As with that with the 2-step aminolysis treatment comparisons, the 1-step aminolysis comparisons displayed statistical significance in peak area between the pre-electrospun solution samples and electrospun mesh samples. This indicates that amine-group functionalization of PCL is not lost in the final electrospun mesh products.

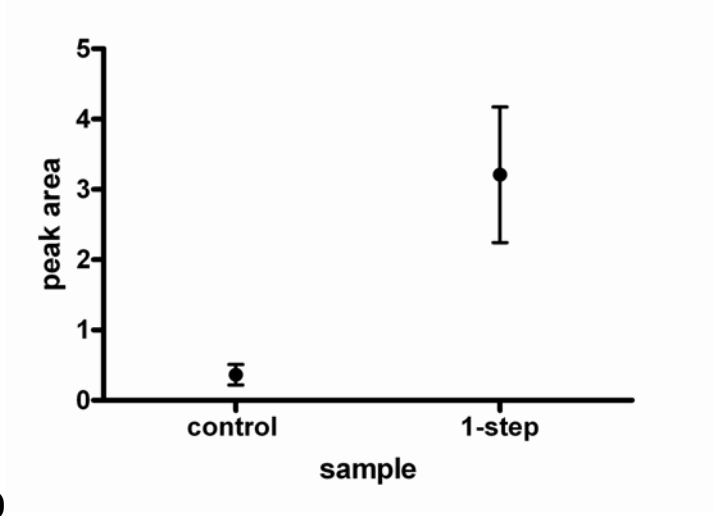
peak area
5
4
3
2
1
0
control
1-step
sample

(a)

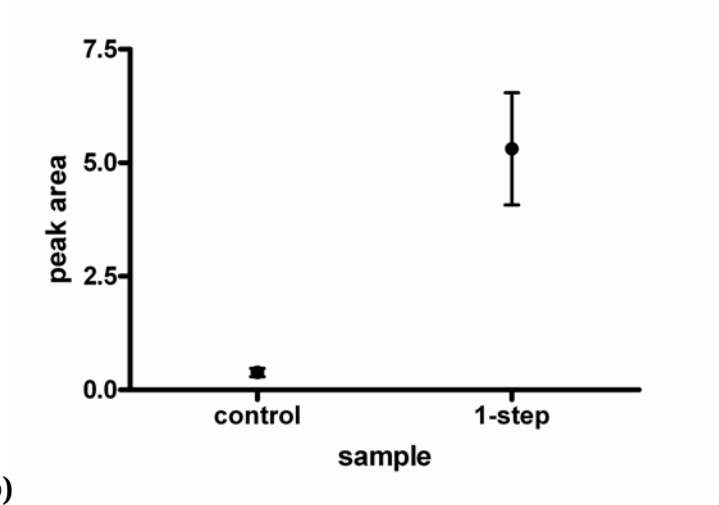
peak area
7.5
5.0
2.5
0.0
control
1-step
sample

(b)

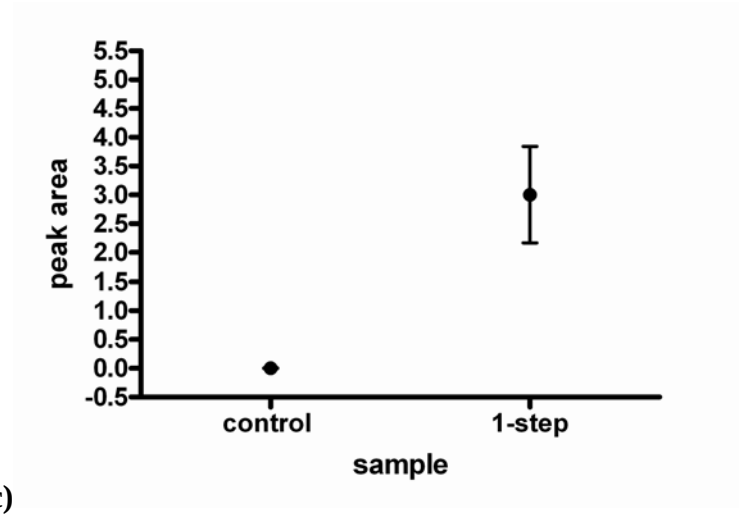
peak area
5.5
5.0
4.5
4.0
3.5
3.0
2.5
2.0
1.5
1.0
0.5
0.0
-0.5
control
1-step
sample

(c)

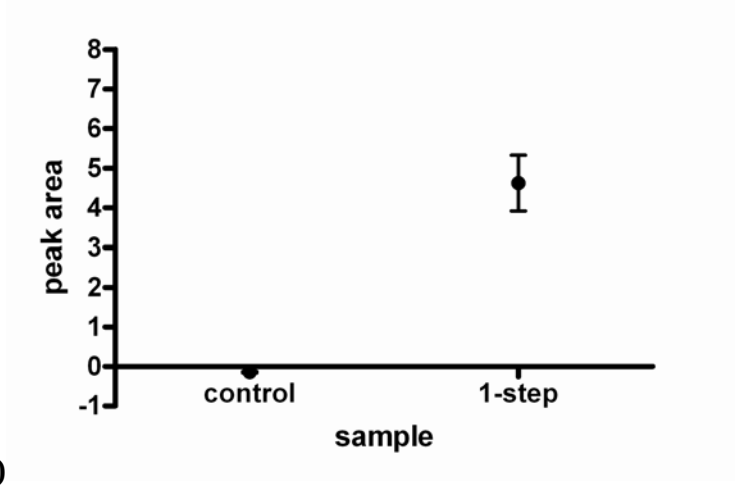
8
7
6
5
4
3
2
1
0
-1
peak area
control
1-step
sample

(d)

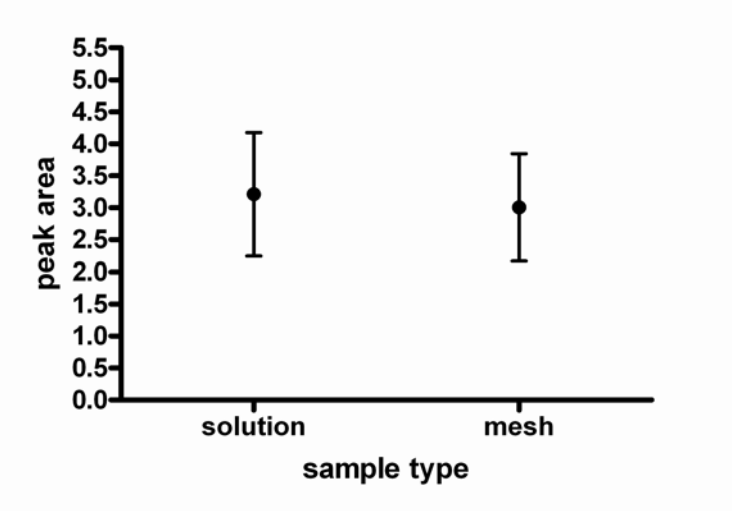
5.5
5.0
4.5
4.0
3.5
3.0
2.5
2.0
1.5
1.0
0.5
0.0
peak area
solution
mesh
sample type

(e)

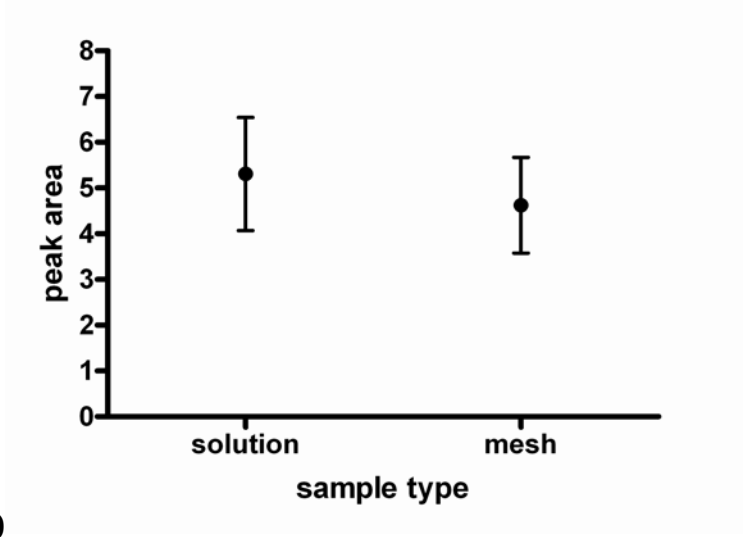

(f)

Figure 16: 1-step aminolysis peak areas for (a) control to 1-step peak 1 area solution comparison, (b) control to 1-step peak 2 area solution comparison, (c) control to 1-step peak 1 area mesh comparison, (d) control to 1-step peak 2 area mesh comparison, (e) 1-step solution to mesh peak 1 area comparison, (f) 1-step solution to mesh peak 2 area comparison.

Table 3: Unpaired two-tailed t-test p-values and sample peak areas for Figure 16. (P-values <0.05 are significant

Test Group	Mean P-value	Sample 1 Peak Area	Sample 2 Peak Area
control to 1-step peak 1 area solution comparison	0.1076	0.3658 ± 0.1458 N=2	3.209 ± 0.9649 N=3
control to 1-step peak 2 area solution comparison	0.0539	0.3830 ± 0.09000 N=2	5.307 ± 1.235 N=3
control to 1-step peak 1 area mesh comparison	0.0102	0.0020 ± 0.006957 N=5	3.004 ± 0.8385 N=6
control to 1-step peak 2 area mesh comparison	0.0026	-0.1444 ± 0.02987 N=5	4.624 ± 1.045 N=6
1-step solution to mesh peak 1 area comparison	0.8863	3.209 ± 0.9649 N=3	3.004 ± 0.8385 N=6
1-step solution to mesh peak 2 area comparison	0.7047	5.307 ± 1.235 N=3	4.624 ± 1.045 N=6

5.3.5 1-Step FT-IR Peak Area Analysis with Decellularized Tissue

The data recorded in Figure 17 shows the results from the 1-step aminolysis test study with decellularized porcine diaphragm. The graphs represent the peak area analysis for the two peaks falling in the 3201-3423 cm^{-1} and 1508-1660 cm^{-1} range, respectively. The comparison includes five control electrospun PCL meshes, five 1-step aminolysis electrospun meshes, and five delaminated 1-step meshes originally attached to the decellularized porcine diaphragm samples.

The control electrospun meshes were derived from an 8% w/v PCL in 50% (v/v) acetone to chloroform solution. The 1-step electrospun meshes and the 1-step delaminated meshes came from the same 10% w/v PCL in 20% (v/v) EDA to chloroform stock solutions. The 1-step aminolysis meshes were scanned with the FT-IR upon formation, while the delaminated 1-step aminolysis samples were scanned approximately 3 days post-formation, when it was discovered that they had physically detached from the decellularized tissue samples. A one-way analysis of variance and a Bartlett's test was conducted for the data sets form Figure 17 and reported in Table 4. The 1-way ANOVA shows statistical significance ($P<0.05$) among treatment group wavenumber peak area means. Similarly, the Bartlett's test shows statistically significance for both peak area ranges as well, further supporting the data for the 1-way ANOVA. Essentially, the 1-step aminolysis shows that amine-group functionalization of PCL does occur upon electrospun formation, but is not present in the older delaminated samples. The FT-IR peak area graphs show that the delaminated samples have nearly identical characteristics to the control samples.

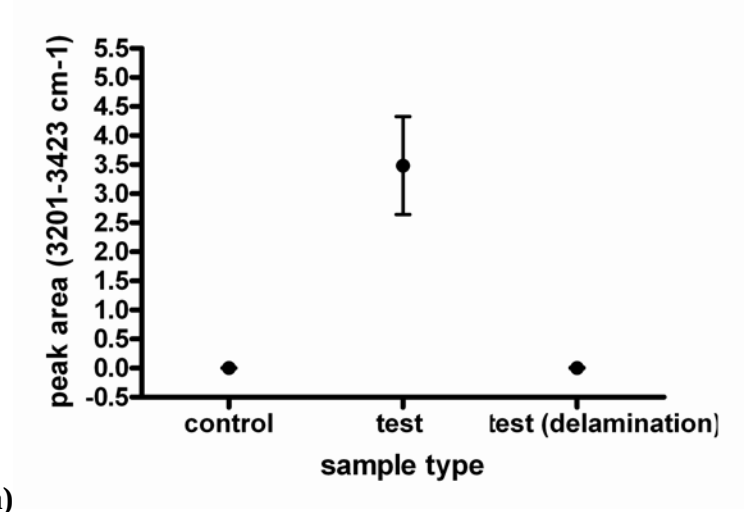

(a)

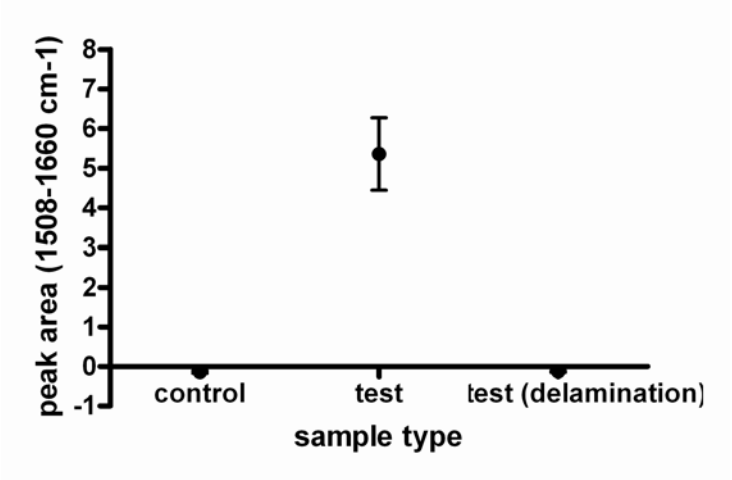

(b)

Figure 17: 1-step aminolysis FT-IR peak area analysis with decellularized porcine diaphragm for (a) peak 1 electrospun mesh samples and (b) peak 2 electrospun mesh samples

Table 4: One-way Analysis of Variance P-values and Bartlett's Test P-values for Figure 17. (P-values <0.05 are significant)

Test Group	1-way ANOVA P-value	Bartlett's test P-value
peak 1 electrospun mesh samples	0.0003	P<0.0001
peak 2 electrospun mesh samples	P<0.0001	P<0.0001

5.3.6 2-Step to 1-Step Aminolysis FT-IR Peak Area Comparison

The graphs in Figure 18 show the direct peak range area comparison of the 2-step aminolysis method to the 1-step method. Essentially, the pre-electrospun solution samples and electrospun meshes samples for both methods were compared to determine if one aminolysis method was more effective than the other.

Table 5 lists the 1-way ANOVA for the data sets from Figure 18. The mean wavenumber peak areas for both the 2-way and 1-way aminolysis treatment group electrospun meshes were found to be significantly different from the control group electrospun meshes. However, the differences among the pre-electrospun solution treatment groups were not statistically significant. Graphically, it appears that the wavenumber peak area mean for the 1-way aminolysis treatment group is higher than the 2-way aminolysis treatment group, but the variances within each group is too high for the area means to vary significantly. Further testing of more samples may be needed to ascertain whether or not differences can be found between the two aminolysis treatment groups.

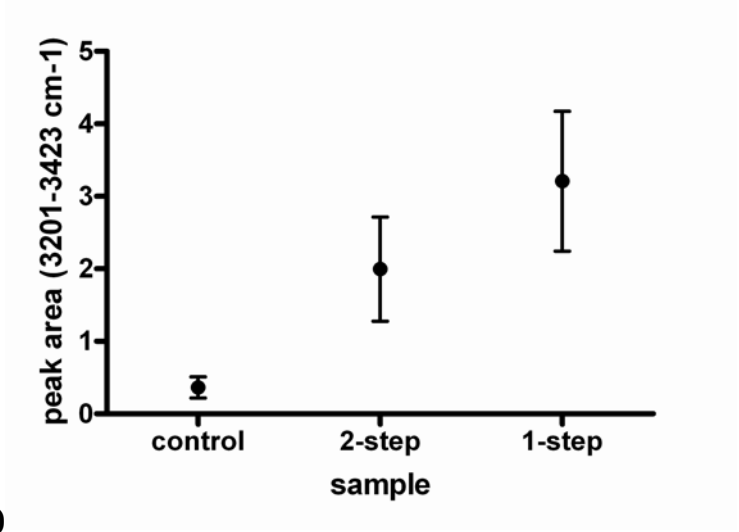

(a)

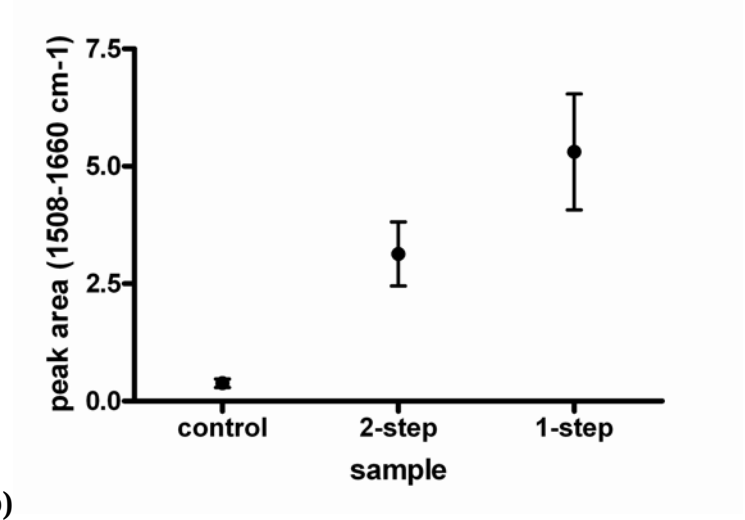
peak area (1508-1660 cm-1)
7.5
5.0
2.5
0.0
control
2-step
1-step
sample

(b)

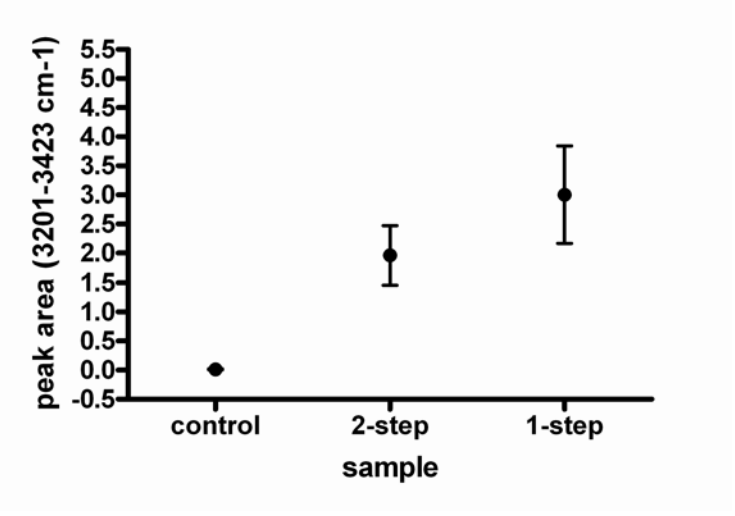
peak area (3201-3423 cm-1)
5.5
5.0
4.5
4.0
3.5
3.0
2.5
2.0
1.5
1.0
0.5
0.0
-0.5
control
2-step
1-step
sample

(c)

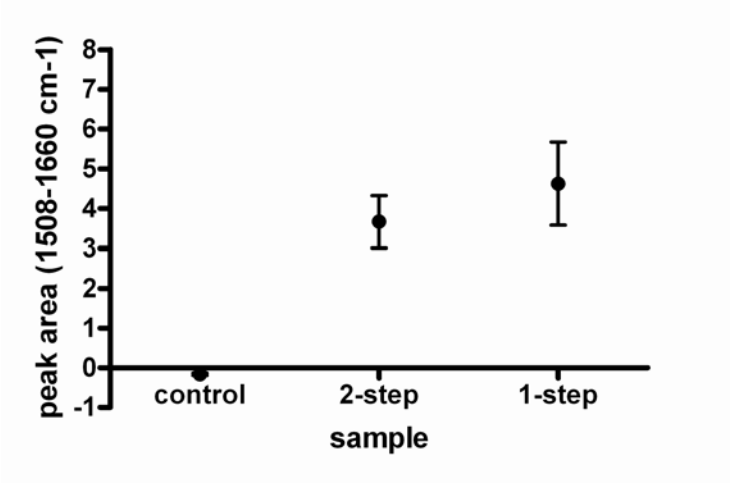

(d)

Figure 18: FT-IR peak area for 2-step and 1-step aminolysis including (a) solution peak 1 comparison, (b) solution peak 2 comparison, (c) electrospun mesh peak 1 comparison, and (d) electrospun mesh peak 2 comparison.

Table 5: One-way Analysis of Variance P-values for Figure 18. (P-values <0.05 are significant)

Test Group	1-way ANOVA P-value
solution peak 1 comparison	0.1540
solution peak 2 comparison	0.0456
electrospun mesh peak 1 comparison	0.0029
electrospun mesh peak 2 comparison	0.0003

5.4 Conclusion

The results from the aminolysis experiments warrant further investigation. The preliminary investigation shows that both aminolysis treatments protocols vary significantly in both of the cited wavenumber peak area ranges compared to the control samples. Specifically, the electrospun meshes from both the 1-step and 2-step aminolysis treatment groups vary significantly in regard to the selected wavenumber peak range areas when compared to the control group electrospun meshes. It is interesting to point out the pre-electrospun solutions comparisons were not significant for all treatment groups and peak area ranges. While the differences between pre-electrospun solutions and meshes were not significant for any sample treatments, the mean peak area ranges were often times lower for the solutions compared the meshes. This coupled with the low number of samples in some treatment groups may have caused the lack of statistical significance between the 1-step and 2-step aminolysis treatment solutions and the control PCL solutions.

It should be noted that all of the samples included in the 2-step aminolysis treatment samples listed in the above graphs were re-dissolved in a 50% (v/v) acetone to chloroform solution before electrospinning. Chloroform was eventually used as a replacement solvent since it was found to re-dissolve the precipitate more effectively; however, not enough data was collected for a statistical analysis to be performed to test for effectiveness. Due to project time constraints and the implementation of 1-step aminolysis protocol, extensive analysis with the 2-step chloroform solvent was abandoned. Additionally, all of the 1-step aminolysis samples cited in the above data used the 20% v/v EDA solvent as opposed to the 40% EDA solvent. The 40% solvent

would not produce electrospun fibers in the 1-step method. Qualitatively, it was determined that the 40% v/v EDA pre-electrospun solutions caused too much loss of viscosity and therefore were ineffective in producing fibers.

The results from the mesh aminolysis experiments were not cited here due to lack of amine group peaks for the listed peak area ranges. Both the Gabriel et al. (2006) and the Zhu et al. (2002) protocols did not reliably affect absorbance spectra of electrospun PCL meshes. One possibility is that the post-electrospun aminolysis treatments only aminolysed the surfaces of the electrospun meshes, resulting in a low population density of amine-functional groups. Thus, the FT-IR sensitivity may have been too high to detect any variation in sample composition. Another possibility is that surface aminolysis did occur to a high degree, but the subsequent electrospun mesh washings cause the aminolysis material to detach for the bulk mesh. The data analysis for both mesh aminolysis experiments can be viewed in the Appendix 2.

CHAPTER 6

FUTURE WORK

Much has been accomplished during the course of this investigative study, but much work remains if a working bionanocomposite hernia repair mesh prototype is to be fully developed. Electrospinning and amine-group functionalization with PCL were reliably demonstrated independently; however, incorporating the functionalized electrospun PCL fibers into a decellularized tissue scaffold is problematic. Originally, it was hoped that electrospun PCL fibers would be uniformly distributed throughout the entire thickness of the decellularized tissue scaffold. Unfortunately, even sub-micron diameter fibers do not appear to penetrate into the tissue matrix. The problem lies not with the fiber diameters, but with the length of the fibers. Hypothetically, the PCL fibers are electrospun continuously, producing an indefinite fiber length and thus an increased surface area to volume ratio. With a high surface area to volume ratio, it becomes nearly impossible for the fiber to penetrate deep into the tissue scaffold due to increased friction. At best, the current method permits the amine-functionalized electrospun PCL fibers to superficially penetrate the decellularized porcine diaphragm tissue samples, which may serve as an adhesion barrier for the hernia mesh implant. However, the preliminary investigative study coupling the electrospun fibers to the decellularized tissue samples indicated that the fibrous films would inevitably detach from the tissue samples. This may be due to lack of physical connections between the fibrous mesh and decellularized tissue, which would inhibit chemical crosslinking as well. Another possibility is that sufficient chemical crosslinking does occur, but the chemical linkage is lost as the functionalized PCL fibers are degraded.

In order to improve the effectiveness of the functionalized electrospun PCL fibers for use in a bionanocomposite material, a couple of issues need to be addressed. First, a time study to test the functionalization of the electrospun fibers needs to be completed. If significant losses in functionalization do occur within a short duration, a new functionalization method may need to be investigated. Optimally, loss in functionalization should closely correlate with the overall fiber degradation rates. Similarly, if the aminolysis process does induce a quicker degradation of the electrospun fibers, then it may not be suitable for the bionanocomposite hernia repair mesh. Secondly, a new method should be developed to incorporate the electrospun fibers into an integrated bionanocomposite tissue scaffold, since the current method does not permit fiber penetration into the matrix. One idea includes the sectioning and subsequent layering of the decellularized diaphragm samples. Layering would allow the functionalized electrospun PCL fibers to be placed throughout the bio-scaffold. Sufficient chemical crosslinking between the fibers and decellularized tissue could produce a durable bionanocomposite material with fairly uniform properties throughout. Of course, concern with any layering method is the potential for delamination once implanted.

Although research with this project has exposed problems that conflict with the original conception for the bionanocomposite hernia repair material, much has been learned in the process. Hopefully the lessons learned from this research can be applied to future work with electrospinning, polymer functionalization, and bionanocomposite materials.

APPENDIX 1

PREPARATION OF THE BIONANOCOMPOSITE

Porcine diaphragm decellularization[5, 63]

The following protocol was used in order to decellularize harvested porcine diaphragm tendon for use in the bionanocomposite. The protocol was modified from an article published by Cartmell et al.

1. Harvest diaphragm tissue and remove diaphragmatic muscle so that only the collagenous central tendon portion remains.
2. Place immediately into Tris buffer solution (pH 8.0) containing 5 mM ethylenediaminetetraacetic acid (EDTA), 0.4 mM phenylmethanesulfonyl fluoride (PMSF), and 0.2% (w/v) sodium azide and store at 4 ºC until ready to use.
3. Place 4 cm x 4 cm piece of tissue to be decellularized into 150 mL Tris buffer solution (pH 8.0) containing 5 mM ethylenediaminetetraacetic acid (EDTA), 0.4 mM phenylmethanesulfonyl fluoride (PMSF), 0.2% (w/v) sodium azide, and 1% (v/v) tri-n-butyl phosphate (TnBP) in a 250 mL flask.
4. Place flask on shaker table at room temperature for 24 hours at 225 rpm.
5. Rinse tissue with 150 mL distilled water in a 250 mL flask on shaker table at room temp. for 24 hours at 225 rpm.
6. Rinse tissue with 100 mL 70% (v/v) ethanol in a 250 mL flask on shaker table at room temperature for 24 hours at 225 rpm.

Crosslinking decellularized tissue[5, 64-66]

Once the porcine diaphragm tissue has been effectively decellularized, subsequent treatments prepare the tissue for chemical crosslinking with the amine-functionalized electrospun PCL fibers. The following protocol procured by communications with Corey Costello Deeken and adviser is a conglomeration from articles by Billiar et al., piercenet.com, and Hermanson et al., respectively.

1. Make a 50% (v/v) acetone to 1x phosphate buffered saline (PBS) solution and adjust pH to 7.2-7.5 range.
2. Make buffer containing 0.1M 2-(N-Morpholino)ethanesulfonic acid (MES) with 0.5M NaCl (pH ~ 6.0).
3. Measure out 1-ethyl-3-[3-dimethylaminopropyl]carbodiimide (EDC) and N-Hydroxysuccinimide (NHS) (2 mM and 5 mM respectively based on total volume of solution needed, typically need 50 mL for each 4 cm x 4 cm piece of tissue).
4. Add EDC to MES buffer, mix well.
5. Add NHS to dimethylformamide (DMF), mix well.
6. Combine EDC and NHS solutions, mix well, and then add to acetone/PBS solution.
7. React 15 min at room temperature
8. Add 50 mL crosslinking solution to each piece of tissue
9. Electrospin directly unto the crosslinked tissue sample using the 1-step PCL aminolysis protocol outline in Chapter 5.
10. Compress electrospun fibrous film/crosslinked tissue with 5 lb weight for 10 minutes.
11. Incubate at room temp overnight on shaker table at 135 rpm.

12. Rinse with 1x PBS at room temp for 48 hours at 225 rpm, changing PBS once.

APPENDIX 2

FT-IR RESULTS OF ELECTROSPUN PCL MESH POST-FUNCTIONALIZATION AMINOLYSIS

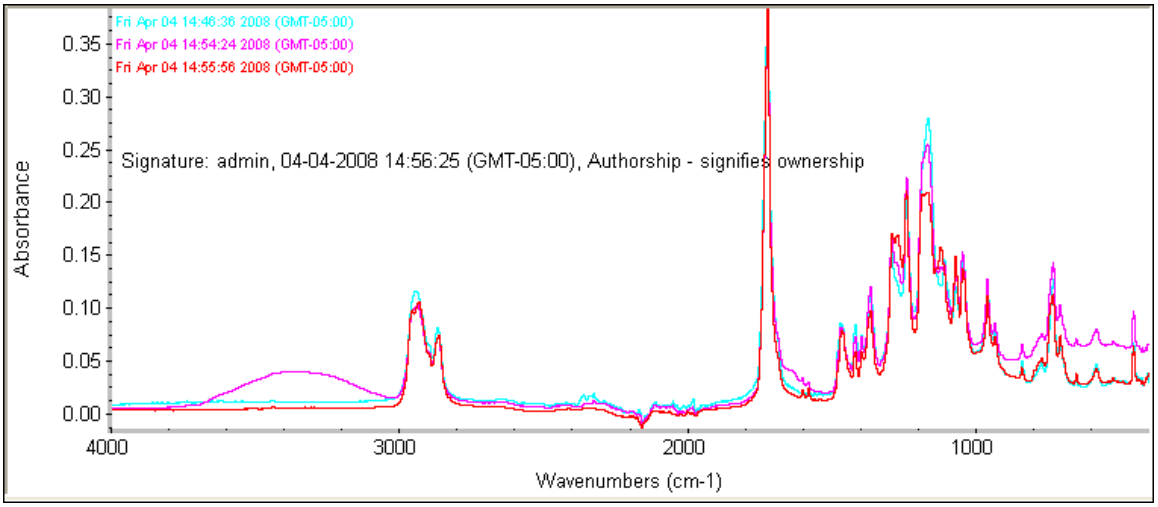

Untreated electrospun PCL meshes (n=3)

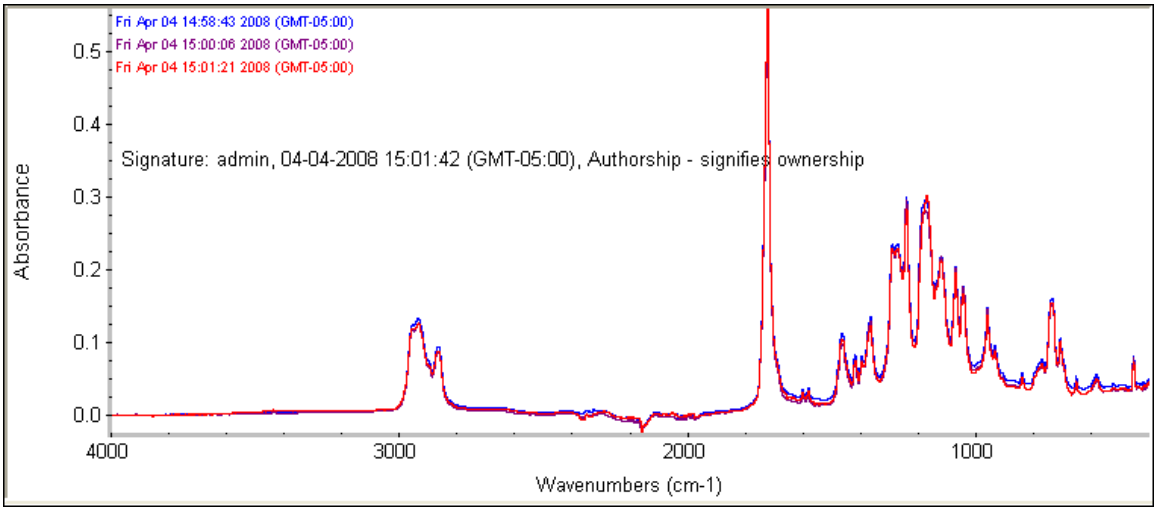

Electrospun PCL meshes treated with 10% v/v EDA in ddH2O (n=3)

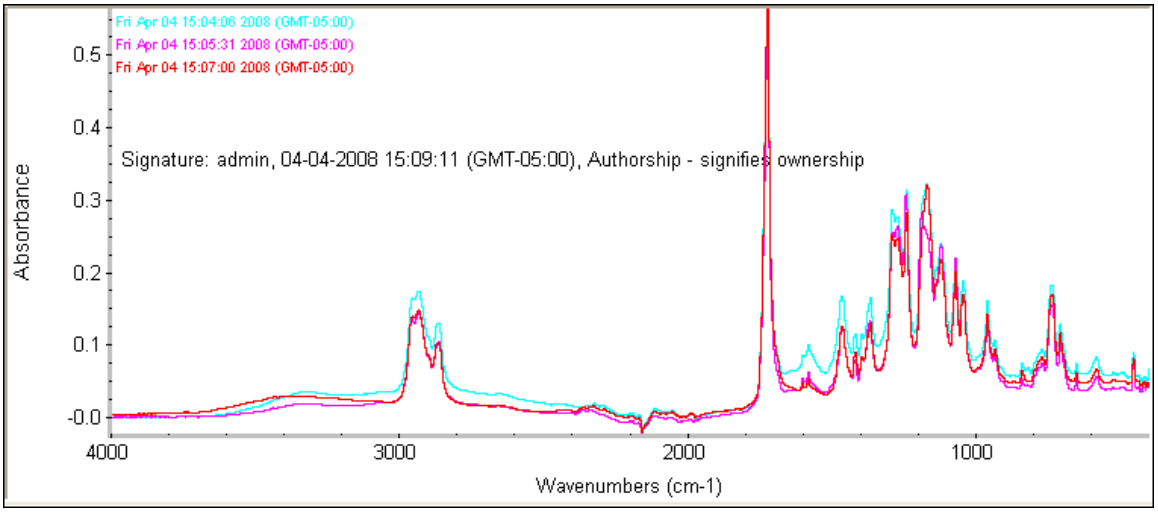

Electrospun PCL meshes treated with 20% v/v EDA in ddH2O (n=3)

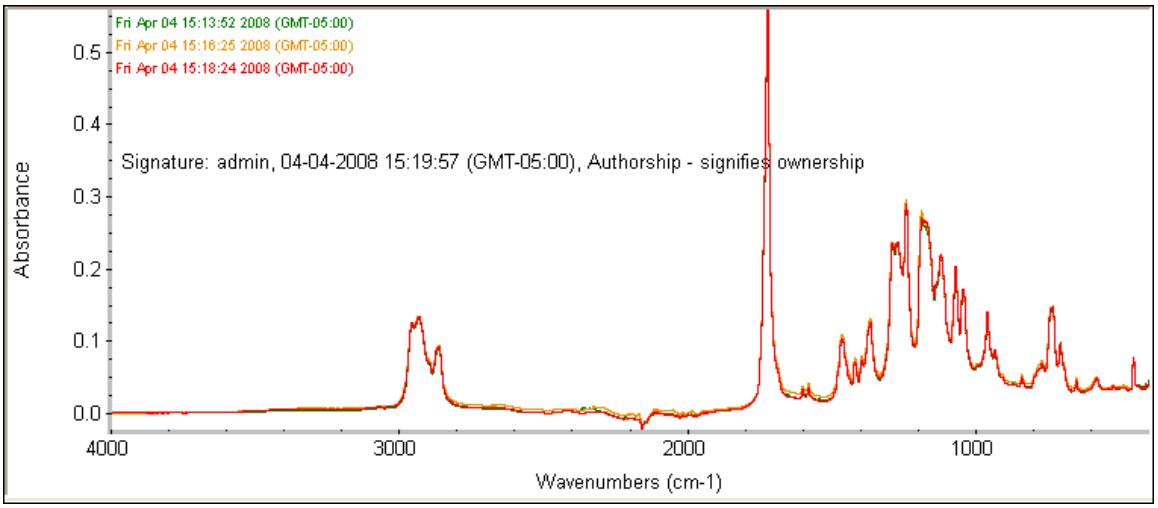

Electrospun PCL meshes treated with 30% v/v EDA in ddH2O (n=3)

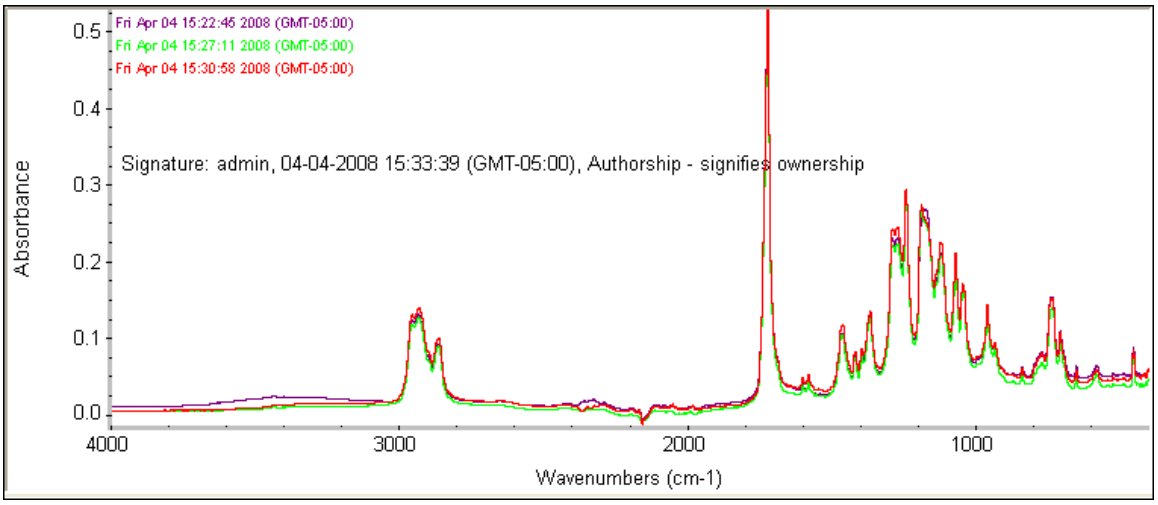

Electrospun PCL meshes treated with 40% v/v EDA in ddH2O (n=3)

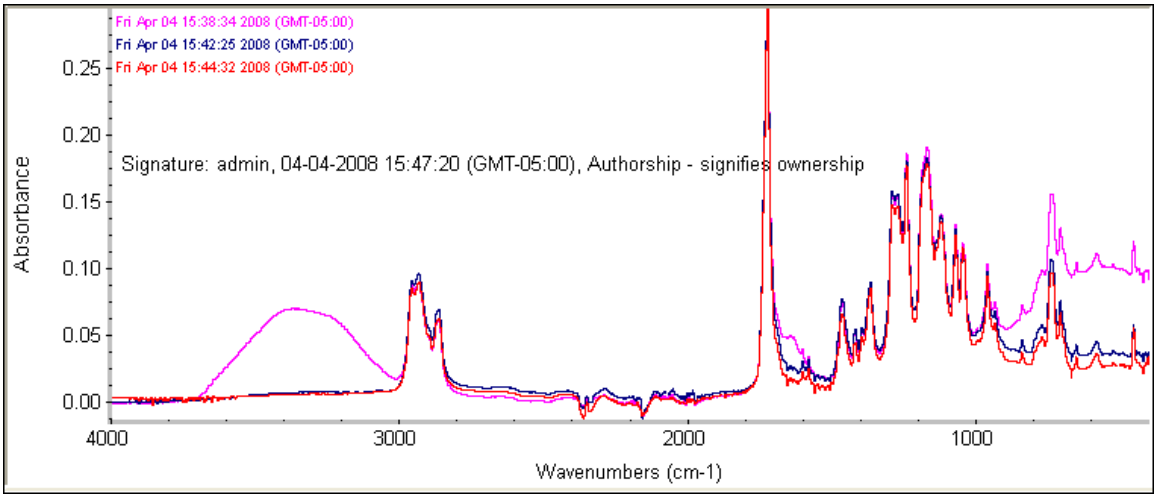

Electrospun PCL meshes treated with 50% v/v EDA in ddH2O (n=3)

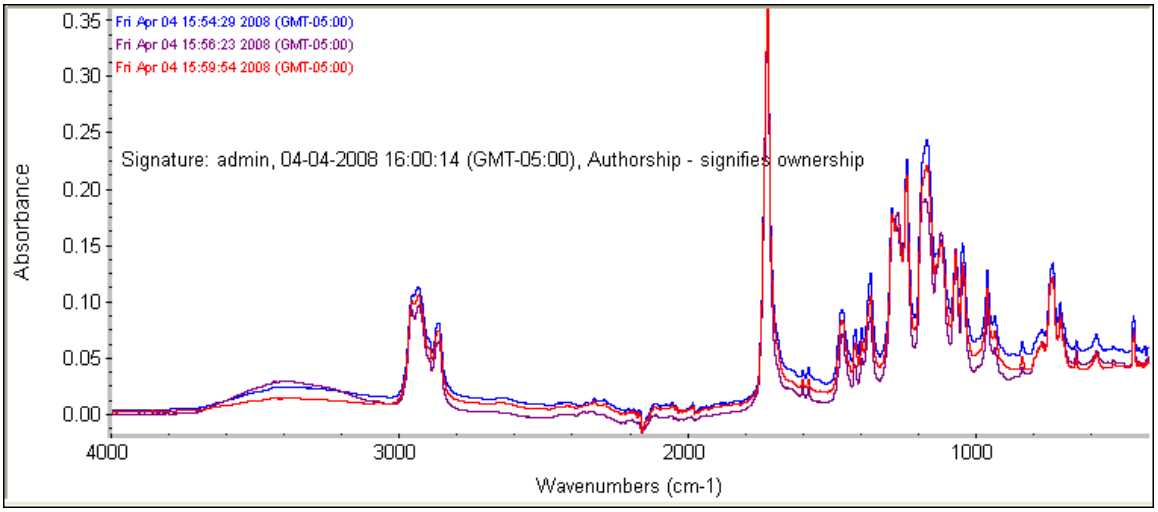

Electrospun PCL meshes treated with 75% v/v EDA in ddH2O (n=3)

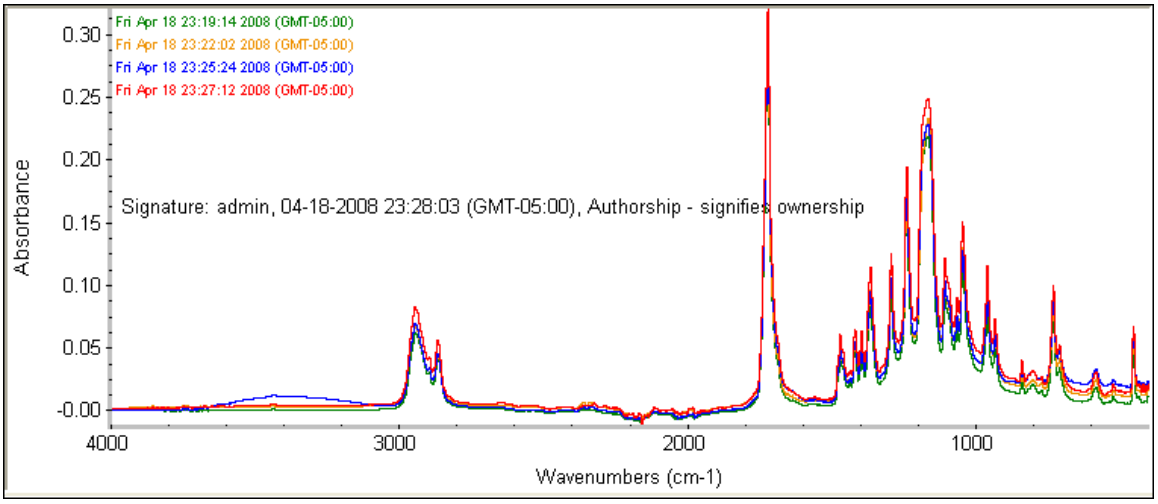

Electrospun PCL meshes treated with 10% wt HDA in isopropyl alcohol (n=3)

Discussion:

The results from both the EDA and HDA mesh protocols yielded inconclusive results. A few samples had a broad FT-IR peak in the 3201-3423 cm^{-1} (peak 1) range; however, none of the samples had an FT-IR peak in the 1508-1660 cm^{-1} range. The significance of the peak 1 in these graphs is very questionable and unsubstantial because the control meshes show evidence of this peak as well. The broad 3201-3423 cm^{-1} range peak present in these samples may have been caused by -OH group stretching vibrations in the FT-IR spectra due to residual ddH2O after washing. Additionally, the utility of post-functionalization electrospun PCL mesh treatment causes the meshes to become stiff and brittle, which would likely limit their use as an implantable material.

APPENDIX 3

DEGRADABLE POLYMER COMPARISON BETWEEN PCL, PLA AND P(L-CO-CL)

Essential Background

Polycaprolactone (Aldrich), Poly(DL-lactide-co-caprolactone) (Aldrich) and Polylactic Acid (Fluka) were compared in a side by side analysis for the effectiveness of the aminolyzing agents 1,6-diaminohexane (HDA) and ethylenediamine (EDA), respectively. For each group, (PCL, P(L-co-CL), and PLA) three separate 3 ml electrospinning solutions were prepared at 10% w/v concentrations. The first two solutions contained a 0.06 g/ml concentration of HDA and EDA, respectively, and the third solution in each group was a control. Each sample was electrospun using an 18 gauge blunt-end needle, 20 kV potential, 20 cm needle tip to collecting plate separation distance, and a variable flow rate that defaulted at 2 ml/ hr. The samples were collected on 1x3" microscopes slides. The slides were each examined using a 150x magnification using a microscope equipped with a digital camera. The sample slides were then soaked in a ddH2O bath for ~2.5 hours, dried with an air hose, and then analyzed with the FT-IR for absorbance spectra analysis.

Solution Table and Experimental notes:

Polymer/ Concentration	Solvent Composition	Aminolyzing Solution	Notes
1) 10% w/v PCL	1:1 v/v chloroform to acetone	0.06 g/ml 1,6-hexanediamine	*1.385 ml chloroform, 1.385 ml acetone, 0.23 ml HDA *total of 0.30 ml solution expelled *collected material began as "spider web" fibers that rose towards needle, then form as a semi opaque fibrous film *solution flow rate ~2 ml/ hr
2) 10% w/v PCL	1:1 v/v chloroform to acetone	0.06 g/ml ethylenediamine	*1.4 ml chloroform, 1.4 ml acetone, 0.2 ml EDA *~0.31 ml solution expelled *formation of a white fibrous film *optimal flow rate was ~4 ml/ hr
3) 10% w/v PCL	1:1 v/v chloroform to acetone	----------	*1.5 ml chloroform, 1.5 ml acetone *~0.3 ml solution expelled *formation of fibrous film begins as flow rate is increased to ~4 ml/ hr
4) 10% w/v P(CL-co-LA)	1:1 v/v chloroform to acetone	0.06 g/ml 1,6-hexanediamine	*1.385 ml chloroform, 1.385 ml acetone, 0.23 ml HDA *~0.78 ml solution expelled (not as much collection on slide) *no visible fiber deposition, more like a gaseous spray *adjustments were made with parameters with no success
5) 10% w/v P(CL-co-LA	1:1 v/v chloroform to acetone	0.06 g/ml ethylenediamine	*1.4 ml chloroform, 1.4 ml acetone, 0.2 ml EDA *~0.58 ml solution expelled *no visible fiber formation, just a translucent film *adjusted all parameters, but no fiber formation
6) 10% w/v P(CL-co-LA	1:1 v/v chloroform to acetone	----------	*1.5 ml chloroform, 1.5 ml acetone *~0.3 ml solution expelled *white fibrous film formation after increasing rate to *4 ml/ hr, fibrous film at 8 ml/ hr
7) 10% w/v PLA	Anhydrous dichloromethane	0.06 g/ml 1,6-hexanediamine	*2.77 ml anhydrous dichloromethane, 0.23 ml HDA *~0.61 ml solution expelled *semi-opaque film forms on slide *flow rate best between 2-4 ml/ hr *not much "substance" is deposited on slide
8) 10% w/v PLA	Anhydrous dichloromethane	0.06 g/ml ethylenediamine	*2.8 ml anhydrous dichloromethane, 0.2 ml EDA *~0.45 ml solution expelled *electro-spray deposited onto slide as opaque film *not much "substance" to film
9) 10% w/v PLA	Anhydrous dichloromethane	----------	*3.0 ml anhydrous dichloromethane *~0.48 ml solution deposited -intermittent opaque fibers deposited on slide *solution dries very quickly on needle tip *4 ml/ hr best flow rate for fiber formation

PCL FT-IR and Microscope

Solution 1- blue

Solution 2- purple

Solution 3- red

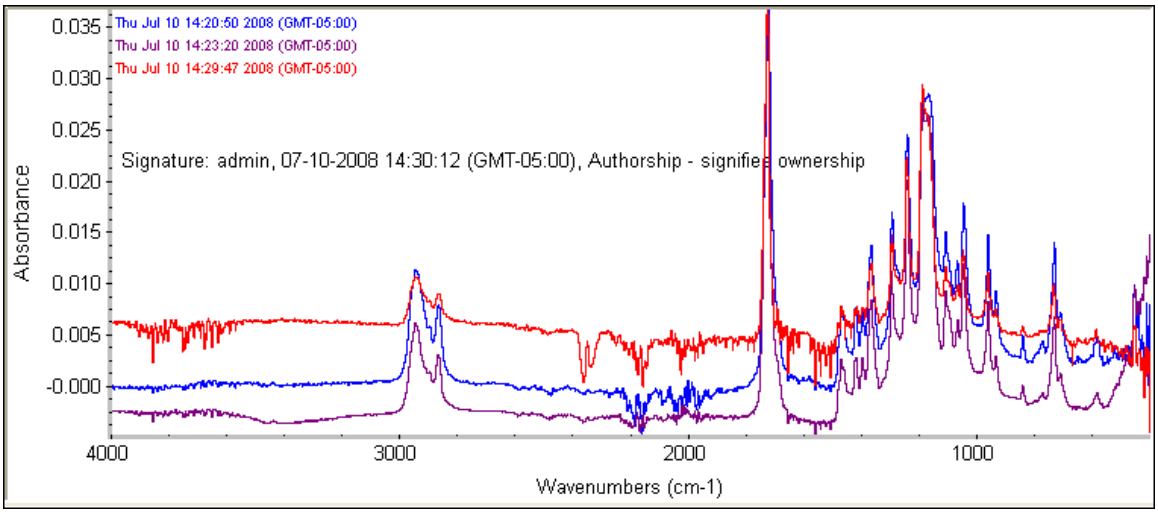

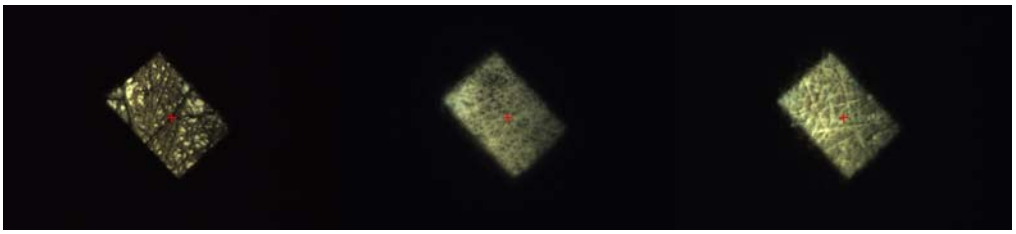

Solution 1 Solution 2 Solution 3

P(L-co-CL) FT-IR and Microscope

Solution 4- teal

Solution 5- purple

Solution 6- red

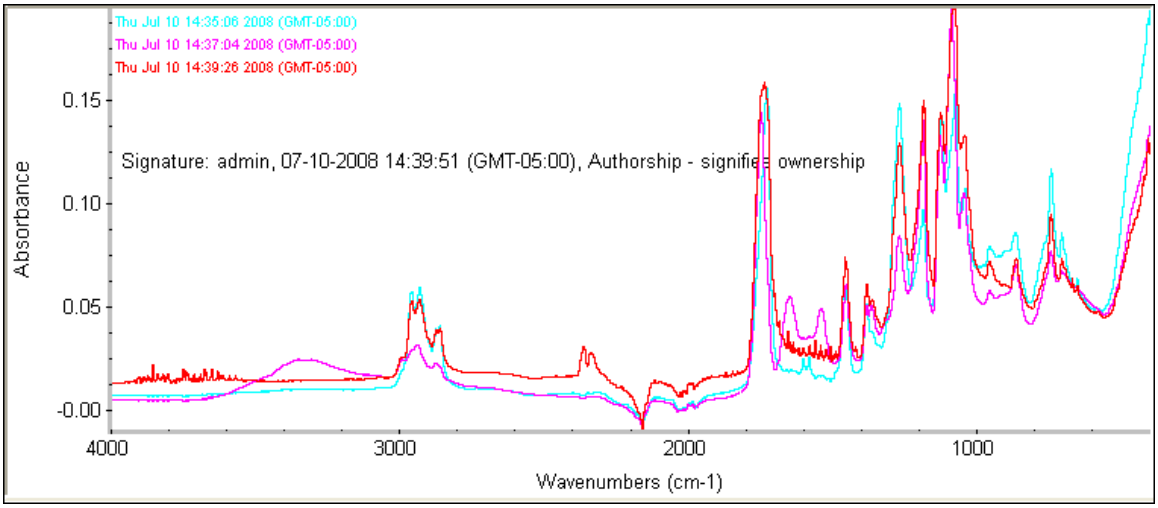

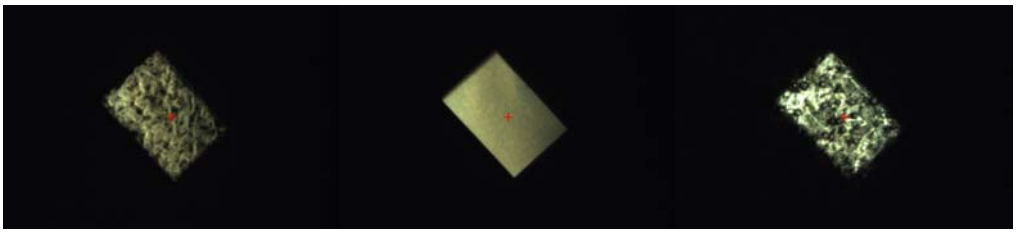

Solution 4 Solution 5 Solution 6

PLA FT-IR and Microscope

Solution 7- green

Solution 8- gold

Solution 9- red

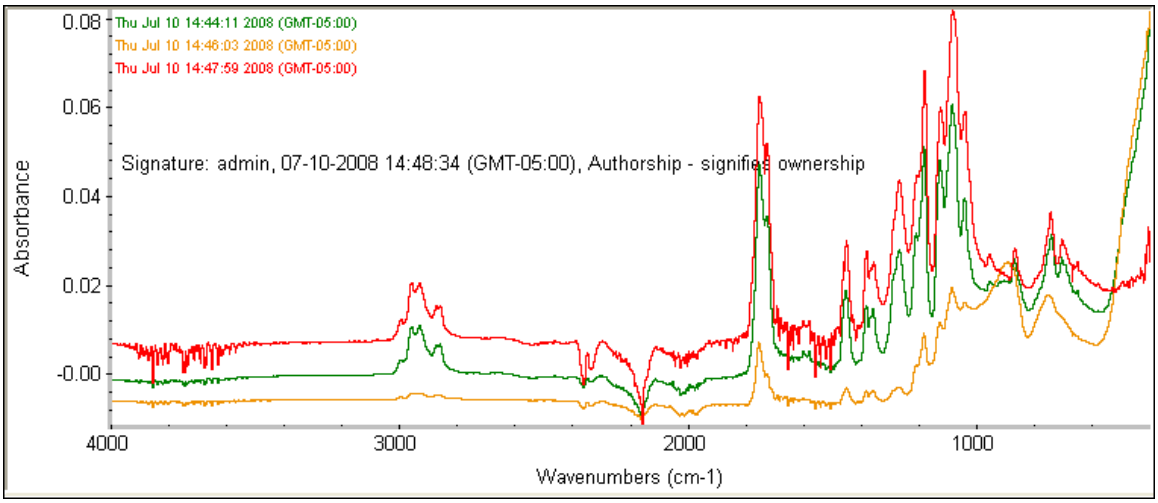

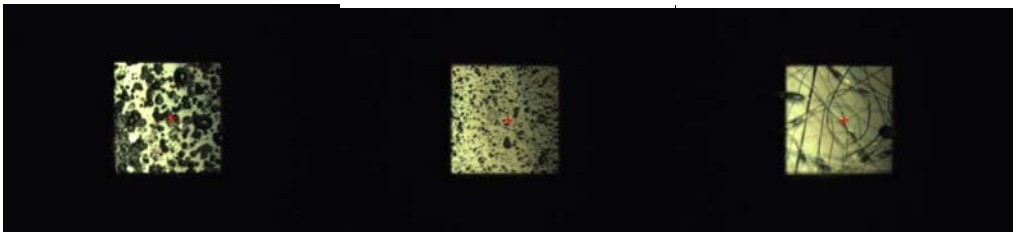

Solution 7 Solution 8 Solution 9

Summary

Electrospinning solution parameters and apparatus parameters for the three experimental groups were standardized based on preliminary qualitative data performed before this experiment. Qualitatively, the results from this experiment show that electrospun fibers are formed with all three PCL electrospinning solutions and with the

control PLA solution. The two PLA aminolysis solutions and all three P(L-co-CL) solutions did not form fibers upon electrospinning. The FT-IR data from this experiment was inconclusive. The only sample that displayed characteristic amine peaks was the P(L-co-CL) aminolysis solution treated with EDA. However, this solution was collected as a film; therefore it is possible that EDA may have been present in the washed sample. It is interesting to note the PCL aminolysis samples did not show amine peaks with the FT-IR, but the EDA solution concentration in this experiment was not the same as in previous "successful" PCL aminolysis experiments. The goal of this experiment was to compare each polymer side by side. Uniformity in the electrospinning solutions was essential, and compromises concerning solution composition were unavoidable.

REFERENCES

1. Franz M. Hernia 2006(10):462-471.

2. Ramshaw B BS. Surgical Materials for Ventral Hernia Repair. General Surgery News: McMahon Publishing, 2007. pp. 16.

3. Robinson TN CJ, Schoen J, Walsh MD. Surgical Endoscopy 2005(19):1556–1560.

4. Conze J KA, Flament JB, Simmermacher R, Arlt G, Langer C, Schippers E, Hartley M, Schumpelick V,. British Journal of Surgery Society Ltd 2005;92:1488–1493.

5. Costello CR BS, Ramshaw BR, Grant SA,. Journal of Biomedical Materials Research B 2007;B(83):44-49.

6. Klinge U JK, Spellerberg B, Piroth C, Klosterhalfen B, Schumpelick V. J Biomed Mater Res 2002;63:765–771.

7. Matthews BD PB, Pollinger HS, Backus CL, Kercher KW, Sing RF, Heniford BT. J Surg Res 2003;114:126-132.

8. Diaz JJ Jr GB, Dobson JM, Grogan EL, May AK, Miller R, Guy J, O'Neill P, Morris JA Jr. Am Surg 2004;70:396-402.

9. Baptista ML BM, Delaney JP. Surgery 2000;128:86-92.

10. Pans A EP, Dewe W, Desaive C. World J Surg 1998;22:479-483.

11. Badylak S. Transplant Immunology 2004(12):367-377.

12. Thomas W. Gilbert TLS, Stephen F. Badylak. Biomaterials 2006;27:3675–3683.

13. Bernard MP CM, Myers JC, Ramirez F, Eikenberry EF, and DJ P. Biochemistry 1983;22:5213-5223.

14. Exposito JY DAM, Solursh M, Ramirez F. J Biol Chem 1992;267:15559–15562.

15. Martins-Green M BM. Semin Dev Biol 1995;6:149-159.

16. Baldwin HS. Cardiovasc Res 1996;31:E34 –E45.

17. Soiderer EE D.V.M. LGDVM, Kazacos EA D.V.M. Ph.D., and Jason P. Hodde MS, and Ryan E. Wiegand, M.S. Journal of Surgical Research 2004;118:161-175.

18. Schumpelick V KU. 2003;90:1457-1458.

19. Greiner A WJ, Yarin AL, Zussman E,. Appl Microbiol Biotechnol 2006(71):387–393.

20. Formhals A. Process and apparatus for preparing artificial threads. vol. 1,975,504. United States, 1934.

21. Li D XY. Advanced Materials 2004;16(14):1151-1170.

22. Lannutti J RD, Ma T, Tomasko D, Farson D. Materials Science and Engineering C 2007;27:504-509.

23. Zonggang C XM, Fengling Q,. Materials Letters 2007;61:3490-3494.

24. Ramakrishna S FK, Teo W, Lim T, Ma Z. Electrospinning and Nanofibers. Singapore: World Scientific Publishing, 2005.

25. Goki Eda SS. Journal of Applied Polymer Science 2007;106(1):475-487.

26. Mit-uppatham C, Nithitanakul, M. and Supaphol, P. Macromolecular Chemistry and Physics 2004;205:2327-2338.

27. Lyons J, Li, Christopher, Ko, Frank. Polymer 2004;45(22):7597-7603.

28. Yi Xin ZH, Jinfeng Chen, Cheng Wang, Yanbin Tong, Sidong Liu. Materials Letters 2008;62:991-993.

29. Lee JS, Choi, K.H., Ghim, H.D. Kim, S.S., Chun, D.H., Kim, H.Y., Lyoo, W.S. Journal of Applied Polymer Science 2004;93:1638-1646.

30. Zong X, Kim, K., Fang, D., Ran, S., Hsiao, B. S., Chu, B. Polymer 2002;24:4403-4412.

31. Pawlowski KJ, Belvin, H. L., Raney, D. L., Su, J., Harrison, J. S., Siochi, E. J. Polymer 2003;44:1309-1314.

32. Sautter BP. Continuous Polymer Nanofibers Using Electrospinning. Chicago: University of Illinois at Chicago, 2005. pp. 1-27.

33. Royal Kessick JF, Gary Tepper. Polymer 2004;45:2981-2984.

34. Rutledge GC LY, Fridrikh S, Warner SB, Kalayci VE, Patra P,. Electrostatic Spinning and Properties of Ultrafine Fibers. National Textile Center, 2001.

35. Yuan L, Yu, W.H., Kang, E.T., Neoh, K.G. Polymer International in Press 2005.

36. Givens SR GK, Rabolt JF, Chase DB,. Macromolecules 2007;40:608-610.

37. Shao Ping Zhong WET, Xiao Zhu c, Roger Beuerman, Seeram Ramakrishna , Lin Yue Lanry Yung ,. Materials Science and Engineering 2007;C(27):262-266.

38. X.M. Mo CYX, M. Kotaki, S. Ramakrishna. Biomaterials 2004;25:1883-1890.

39. Wenguo Cui XL, Shaobing Zhou, Jie Weng. Journal of Applied Polymer Science 2007;103:3105-3112.

40. Ji-Huan He Y-QW. Polymer 2004;45(19):6731-6734.

41. Matthews JA WG, Simpson DG, Bowlin GL,. Biomacromolecules 2002;3:232-238.

42. Ken-Jer Wu C-SW, Jo-Shu Chang. Process Biochemistry 2007;42:669-675.

43. Estelles J, Duenas J, and Cortazar I. Journal of Materials Science-Materials in Medicine 2008;19(1):189-195.

44. Biomaterials Science: An Introduction to Materials in Medicine. In: Buddy D. Ratner ASH, Frederick J. Schoen, Jack E. Lemons, editor. Biomaterials. San Diego, California: Elsevier Academic Press, 2004. pp. 851.

45. Wei Hea ZM, Thomas Yonga, Wee Eong Teoc, Seeram Ramakrishna. Biomaterials 2005;26:7606-7615.

46. Sung In Jeong SYK, Seong Kwan Cho, Moo Sang Chong, Kyung Soo Kim, Hyuck Kim, Sang Bong Lee, Young Moo Lee. Biomaterials 2007;28:1115-1122.

47. Dhirendra S. Katti KWR, Frank K. Ko, Cato T. Laurencin. Wiley InterScience 2004.

48. Jingwei Xie C-HW. Pharmaceutical Research 2006;23(8):1817-1826.

49. Ko Eun Park HKK, Seung Jin Lee, Byung-Moo Min, Won Ho Park. Biomacromolecules 2006;7(1):635-643.

50. Stankus JJ FD, Bladylak SF, Wagner WR,. journal of biomaterial science, polymer edition 2008;19(5):635-652.

51. Riva R, Lenoir S, Jerome R, and Lecomte P. Polymer 2005;46(19):8511-8518.

52. Paola Laurienzo MM, Giuditta Mattia, Gennaro Romano. Macromolecular Chemistry and Physics 2006;207(20):1861-1869.

53. Martina Ka¨ llrot UE, A.-C. Albertsson. Biomaterials 2006;27:1788-1796.

54. Ulrich Hersel CD, Horst Kessler. Biomaterials 2003;24:4385-4415.

55. Santiago LY NR, Rubin JP, Marra KG. Biomaterials 2006;27:2962-2969.

56. Karakecili A SC, Gumusderelioglu M, Marletta G,. J Mater Sci: Mater Med 2007(18):317-319.

57. Taek Gyoung Kim TGP. biotechnol. progress. 2006;22:1108-1113.

58. Zhu Y, Liu X, and Shen J. Biomacromolecules 2002;3(6):1312-1319.

59. Tristan I. Croll AJOC, Geoffrey W. Stevens, and Justin J. Cooper-White. Biomacromolecules 2004;5:463-473.

60. Gabriel M VNAG, Van Hinsbergh VWM, Van Nieuw Amerongen AV, Zentner A,. J. Biomater. Sci. Polymer Edn. 2006;17(5):567-577.

61. Jolene E. Valentin JSB, George P. McCabe and Stephen F. Badylak. J Bone Joint Surg Am 2006;88:2673-2686.

62. Venugopal J and Ramakrishna S. NANOTECHNOLOGY 2005;16(10):2138-2142.

63. Cartmell JS, Dunn M.G. J Biomed Mater Res 2000;49:134-140.

64. Billiar K MJ, Laude D, Abraham G, Bachrach N,. J Biomed Mater Res 2001;56:101-108.

65. http://www.piercenet.com. EDC instructions, Pierce package insert.

66. Hermanson GT. Academic Press 1996:593-596.